

Nucleon - Nucleon Interaction with Instanton Induced Interaction

A Thesis Submitted to Mangalore University
for the Award of the Degree of
Doctor of Philosophy
in
Physics



Submitted by
Vanamali C. S.

Under the Supervision of
Dr. K. B. Vijaya Kumar

Department of Studies in Physics
Mangalore University
Mangalagangothri - 574199
INDIA

July 2017

Declaration

I hereby declare that the matter embodied in this thesis titled **Nucleon - Nucleon Interaction with Instanton Induced Interaction** is original and carried out by me under the supervision of Dr. K. B. Vijaya Kumar, Professor, Department of Studies in Physics, Mangalore University, Mangalagangothri. This work contains no material previously published or written by another person, except where due reference has been made in the text. This work has not been formed the basis for the award of any other degree or diploma in any University or Institution.

Mangalagangothri

July ,2017

Vanamali C S

(Author)

Certificate

This is to certify that the thesis titled **Nucleon - Nucleon Interaction with Instanton Induced Interaction** submitted to Mangalore University by Mr. Vanamali C S, for the award of the degree of Doctor of Philosophy, is a bona fide record of the research work done by him under my guidance. The contents of this thesis in full or part have not been submitted to any other University or Institution for the award of any degree or diploma.

Mangalagangothri

July ,2017

Dr. K. B. Vijaya Kumar

Professor

Department of Studies in Physics

Mangalore University

Mangalagangothri

Acknowledgement

I am grateful to Prof. K. B. Vijaya Kumar for the guidance during the PhD work and afterwards. I thank the Chairman and faculty of the Department of Physics for their constant support. I thank the University for providing me this opportunity. I acknowledge the support of the office staff of the Department as well as the University. I am very much indebted to Raghavendra for the stimulating discussions on everything under the Sun and inside of it. I fondly recollect the good company of P. R. Deepak. I also acknowledge the support of all my friends and colleagues. I am grateful to Mr. Shreedhara Bhat and family for accommodating me for the duration of PhD. Finally, I acknowledge the support of my parents and my family.

List of Publications

In Journals

1. *Nucleon-nucleon interaction with one-pion exchange and instanton-induced interactions*, **C. S. Vanamali** and K. B. Vijaya Kumar, Phys. Rev. C 94 (2016) 054002.

In Conferences

1. *Nucleon-nucleon interaction with one-pion exchange and instanton-induced interactions*, **C. S. Vanamali** and K. B. Vijaya Kumar, Proceedings - DAE Symposium on Nuclear Physics (held at SINP, Kolkata, 05-09 Dec.), Vol 61, (2016), pp 670-671.

Contents

Declaration	i
Certificate	ii
Acknowledgement	iii
List of Publications	iv
1 Introduction	1
1.1 Nucleon-Nucleon Interaction	1
1.2 Phenomenological models	3
1.3 Deep Inelastic Scattering (DIS)	6
1.4 Quantum Chromodynamics (QCD)	7
1.5 QCD inspired Nuclear Models	9
2 The Model	11
2.1 The Hamiltonian	11
2.2 One-Gluon Exchange Potential (OGEP)	12
2.3 Instanton Induced Interaction (III)	14
2.4 One-Pion Exchange Potential (OPEP)	16
2.5 Resonating Group Method (RGM)	17
2.5.1 Wave function of a Nucleon	17
2.5.2 Wave function of a two Nucleon system	18
3 Results and Discussion	23
3.1 Hamiltonian and the Matrix elements	23
3.1.1 Parameters	26
4 Summary and Conclusions	28
4.1 Summary of the work	28
4.2 Scope for future works	29

A	Appendix: Matrix elements	30
A.1	Calculating the Matrix elements in RGM.	30
A.1.1	Spin and Isospin matrix elements	33
A.1.2	Color matrix elements	33
A.1.3	Lists of Matrix elements.	34
B	Appendix: Plots	42
	Bibliography	53

List of Figures

2.1	Tree level diagram for one gluon exchange.	13
B.1	Total kinetic energy.	42
B.2	Direct part of the kinetic energy.	42
B.3	Exchange part of the kinetic energy.	42
B.4	Total Coulomb energy from OGEP.	43
B.5	Direct part of the Coulomb energy from OGEP.	43
B.6	Exchange part of the Coulomb energy from OGEP.	43
B.7	Total color electric energy from OGEP.	44
B.8	Direct part of the color electric energy from OGEP.	44
B.9	Exchange part of the color electric energy from OGEP.	44
B.10	Total color magnetic energy from OGEP.	45
B.11	Direct part of the color magnetic energy from OGEP.	45
B.12	Exchange part of the color magnetic energy from OGEP.	45
B.13	Total energy from color independent part of III.	46
B.14	Direct part of the color independent part of III.	46
B.15	Exchange part of the color independent part of III.	46
B.16	Total color electric energy from III.	47
B.17	Direct part of the color electric energy from III.	47
B.18	Exchange part of the color electric energy from III.	47
B.19	Total color magnetic energy from III.	48
B.20	Direct part of the color magnetic energy from III.	48
B.21	Exchange part of the color magnetic energy from III.	48
B.22	Total contribution from OGEP.	48
B.23	Total contribution from III.	48
B.24	Total OPEP energy.	49
B.25	Direct part of the OPEP energy.	49
B.26	Exchange part of the OPEP energy.	49
B.27	Total Confinement energy.	50
B.28	Direct part of the confinement energy.	50
B.29	Exchange part of the confinement energy.	50
B.30	Direct and exchange parts of the Hamiltonian in the adiabatic limit.	51

B.31 NN potential with OPEP.	52
B.32 NN potential without OPEP.	52

List of Tables

3.1	List of parameters	27
A.1	Different operators of the Hamiltonian	40
A.2	Color, spin and isospin matrix elements	41

Abstract

We have calculated the singlet (1S_0) and triplet (3S_1) Nucleon - Nucleon (NN) interaction potential in the $SU(2)$ nonrelativistic quark model (NRQM) using the resonating group method (RGM). The Hamiltonian consists of the kinetic energy of the quarks, harmonic confinement potential and quark-quark interaction potentials. The interaction potentials include the one-gluon exchange potential (OGEP), the instanton induced interaction (III) potential and the one-pion exchange potential (OPEP). We have studied the contributions of the various parts of the interaction potentials to the NN interaction. We have also examined the effects of the OPEP on the NN interaction.

The RGM treats the nucleons as clusters of three quarks. The exchange of the quarks between the clusters leads to the interaction between these clusters. The RGM divides each component of the Hamiltonian into two components - direct and exchange. The direct component of the Hamiltonian is present everywhere in space - at all nucleon separations, while the exchange components are present only in a short interval of space - at small nucleon separations, where the wave functions overlap significantly. Thus the interaction between the nucleons is described by the exchange part of the Hamiltonian. To obtain the NN interaction potential, we subtract the residual energy at asymptotic distances from the energy obtained. This approximation is called the Born-Oppenheimer approximation or the adiabatic approximation.

The present model successfully reproduces the short range repulsion, intermediate range attraction and the long range saturation properties of the NN interaction. The short range repulsion in the model is primarily due to the color magnetic interactions between the quarks and the kinetic energy of the quarks. The color magnetic interactions arise from one-gluon exchange as well as the III and they distinguish between the 1S_0 and the 3S_1 states. The total contribution of the III is attractive in the short and the intermediate ranges. The total contribution of the OGEP is repulsive in the short and the intermediate ranges. The OPEP gives state independent repulsion in the short and the intermediate ranges. The color electric terms do not contribute to the interaction because the contribution of the color electric terms is nearly the same for the $(0s)^6$ configuration as well as the $2(0s)^3$ configuration of quarks.

The direct part of the Hamiltonian leads to state independent attraction in the short and the intermediate ranges. The contribution of the exchange part of the Hamiltonian to the triplet state shows a small attraction in the intermediate range where as for the singlet state it is completely attractive. The presence of OPEP

removes the intermediate range attraction from the 1S_0 state. Thus, in the presence of OPEP, only the triplet (3S_1) state exhibits intermediate range attraction where as in the absence of the OPEP both the states exhibit intermediate range attraction.

Chapter 1

Introduction

The field of nuclear physics is as old as the discovery of nucleon itself. Ernst Rutherford's alpha scattering experiment established the presence of nucleus in an atom. However, it was not until a few years that the constituents of the nucleus were to become clear. The discovery of neutrons by Chadwick in 1932 brought in new challenges.

A proton is positively charged while a neutron is neutral. This raised questions about the stability of the nucleus. Gravitational force was too weak to hold the electrically repelling protons together. The question of nuclear stability needed a completely unorthodox explanation. This question - even though we know a lot more about the nuclear force today - remains unanswered.

Soon after the neutrons were discovered, Werner Heisenberg introduced the first model of a "Nucleon". It was formulated that the protons and neutrons were multiplets of a degree of freedom similar to that of spin - called the "isospin". This explained the known properties of the nucleons at that time. The protons and neutrons having nearly equal mass was seen as the consequence of them being isospin doublets. But the difference in their charge remained unexplained. We now know through various experiments that the nucleons are made up of strongly interacting particles called quarks which have remained fundamental to the energy scales available at present [1].

1.1 Nucleon-Nucleon Interaction

Various models were proposed to explain the known properties of the nuclei [2]. The models could explain the mass of the nucleons and their electromagnetic moments. But, the real test for these models was the nucleon-nucleon (NN) interaction. The NN interaction potential is calculated from the cross section in the following way:

1. The scattered wave is characterized by the wave function,

$$\psi(\mathbf{r}) = e^{i\mathbf{k}\cdot\mathbf{r}} + f(\theta)\frac{e^{ikr}}{r}$$

where $f(\theta)$ is the scattering amplitude is given by

$$f(\theta) = \sum_l (2l+1) f_l(k) P_l(\cos \theta)$$

where the partial amplitudes $f_l(k) = \frac{e^{i\delta_l}}{k} \sin \delta_l$ and δ_l is the phase shift. The differential scattering cross section is,

$$\frac{d\sigma}{d\Omega} = |f(\theta)|^2$$

Integrating over all Ω and making use of the above expressions, one arrives at the total cross section as,

$$\sigma_T = \frac{4\pi}{k^2} \sum_l (2l+1) \sin^2(\delta_l(k))$$

Thus by decomposing the total cross section into the angular momentum components one can find the corresponding phase shifts.

2. The phase shift can then be used to get the scattering length. Scattering length is defined as,

$$a_0 = -\lim_{k \rightarrow 0} \frac{1}{k} \sin \delta(k)$$

Scattering length gives the radius of the equivalent hard sphere from which a point particle is scattered.

3. The NN system has a bound state if the scattering length is positive. If the scattering length is negative, the state could either be a bound state or a scattering state. From the scattering data, one finds that the scattering length is positive in the triplet channel and negative in the singlet channel.

The NN interaction potential was found to exhibit three major properties:

1. Short range repulsion for separation $r \lesssim 1\text{fm}$,
2. Intermediate range attraction for $1\text{fm} \leq r \leq 2\text{fm}$, and
3. long range saturation for $r \gtrsim 2\text{fm}$.

In addition, NN system resulted in a bound state in the triplet (3S_1) channel and not in the singlet (1S_0) channel. This bound state is called the deuteron. The deuteron possesses interesting properties. It has a binding energy of $\sim -2.224\text{MeV}$. Deuteron is not a pure state - it is a mixture of 3S_1 and the 3D_1 states. This is evident as the quadrupole moment of deuteron is non-zero.

The problem of NN interaction has been studied extensively in the past. The various models used to explain the characteristics of NN interaction can be grouped into: potential models, Boson exchange models, and Effective Field Theories.

1.2 Phenomenological models

Potential models used to explain NN interaction can be broadly divided into phenomenological potential models and QCD inspired potential models. These potentials are either derived from the QCD Lagrangian or constructed based on the symmetries of the NN system. The combined system of two nucleons must possess translational, rotational, spin, and isospin symmetries. Thus any potential constructed to obey these symmetries will contain a central part that depends only on the separation between the nucleons, terms with spin - spin interaction, terms with isospin - isospin interaction, and terms that give spin - orbit coupling and tensor interactions. Of these, the first three preserve rotational, spin, and isospin symmetries. the long range part of the interaction is usually attributed to the tensor terms. One - Pion Exchange (OPE) interaction is assumed to give rise to the long range part of the interaction.

The first theory of NN interaction was given by Hideki Yukawa [3]. Yukawa argued that the protons and neutrons interacted with each other by *exchanging* virtual pions. That the pions are massive implied that the nuclear force is a short range force. The theory predicted that the long range behavior of the NN interaction was due to One - Pion Exchange whereas the short and intermediate range behaviors were due to the exchange of multiple pions. Even though this model failed to predict the physical properties and the dynamics of the pions satisfactorily, the long range behavior of NN interaction derived from this model matched the observed behavior. Various modifications were proposed to this model [4, 5, 6, 7], but all these models failed to reproduce behavior of the NN interaction in the short and the intermediate range as the multi - pion exchange potentials lacked spin - orbit potentials.

It was later shown by Okubo and Marshak that the most general NN interaction potential must contain a central term, a spin - spin interaction, a spin - orbit interaction, a tensor term, a quadratic spin orbit term, a momentum dependent term and the corresponding terms with isospin dependent parts [8].

The first set of potentials that were relatively successful in explaining the NN

scattering cross section were the Hamada - Johnston [9] and the Yale group [10] potentials. The Hamada - Johnston potential consisted of central, spin - orbit, and tensor terms. In the limit of large r , position dependent part of the potential was given by the Yukawa potential. The parameters in the potential were fitted to reproduce the scattering cross section. The potential contained a hard core. This potential was later modified to one with a soft core and to include the difference in the mass of the pions. This modification reproduced the results satisfactorily and eliminated the need for the hard cores. The Yale group potentials consisted of the OPEP in addition to the central, spin - orbit, tensor and the quadratic spin - orbit terms. This potential too has a hard core. Both the above potentials behaved like OPE for orbital angular momentum $l > 5$. The presence of hard core and the very form of these potentials made them unsuitable for many body calculations. The Reid68 [11] and the Reid - Day [12] potentials were proposed to overcome these disadvantages. These potentials were local and static and had soft cores. The Reid68 potential was primarily aimed to solve the two nucleon scattering problem. The Reid - Day potential was the extension of the Reid68 potential to the three nucleon systems. This potential too was a local static potential with a soft core. However, both the potentials failed to satisfactorily reproduce the scattering data as well as the deuteron properties.

To overcome the above limitations, the Paris group potentials were proposed [13]. The Paris group potentials were derived from the dispersion relations and included two pion exchange in addition to OPE and the ρ -meson exchange. The short range part was given by a constant soft core. The pion exchanges were derived from the pion - pion and pion - Nucleon scattering. The model consisted of 12 parameters, all fitted to the existing data. The model failed to explain the short range part of the scattering data and was hard to apply for many body calculations. The modifications introduced later also failed to explain the very low energy scattering ($< 10\text{MeV}$).

The Urbana V14 potential used TPE for the intermediate range, OPE for the long range, and the Wood - Saxon potential for the short range part of the interaction [14]. The model had 14 free parameters. The Argonne potentials [15] were an attempt by the Argonne group to explain the NN interaction. The V14 potential by the Argonne group was a modified version of the Urbana V14 potential. The modification introduced could explain the short range phase shifts more accurately than its predecessor. The V28 potential by the same group included the Δ degrees of freedom in the potential and hence had 28 parameters. This resulted in the inclusion of the $\pi N\Delta$, $\pi\Delta\Delta$, $N\Delta$, and the $\Delta\Delta$ channels in addition to the πNN and the NN channels of the V14 potential. The V18 potential introduced later included the charge - dependence and charge - asymmetry terms in addition to the electromagnetic terms.

The discovery of more heavy mesons led to the introduction of the Boson Exchange models [16]. The short range repulsion was attributed to vector meson (ρ, ω, ϕ) exchanges where as the intermediate range attraction was modeled by the exchange of the scalar σ mesons. The vector mesons were studied in detail theoretically by Breit [17] and Sakurai [18] and their predictions for the mass of the ω meson were confirmed by experiments later. The OBE models explain the short range repulsion between nucleons as the effect of the spin-orbit interaction of the vector meson exchange potential.

The Bonn-group potentials were derived from field theoretic analysis of the NN scattering [19, 20, 21]. The potential included terms arising from the exchange of meson below the pion - production threshold. The exchange of $\pi, \omega, \delta, \rho, 2\pi$, and $\pi\rho$ were taken into account. The potential was derived in the momentum space and was energy dependent. To overcome the complexity of the potential in the configuration space, the $2\pi + \rho$ exchange was replaced by the exchange of the σ meson and the $\pi\rho$ exchange was removed. Also η exchange was introduced to improve the 3P_1 phase shift. The parameters were fitted to explain the np scattering. The model reproduced the NN scattering data accurately up to 300 MeV. The salient features of the model were multiple. Nucleons and mesons were treated on an equal footing in the model. The model also included the meson retardation effects and the off shell behavior of the nucleon. The model could be expanded to analyze the medium effects on NN interaction, the electromagnetic properties of the nuclei and the charge symmetry and charge independence breaking of the interaction. The potential was derived in the momentum space and the parameters were fitted to np scattering only.

Another set of successful potentials were the Nijmegen group potentials [22, 23, 24]. These potentials use meson exchange and QCD degrees of freedom in addition to the phenomenological potentials. The potentials are general in the sense that these potentials describe not only NN interaction but also other baryon - baryon and baryon - anti-baryon interactions.

The success of these potential models led to the development of a family of such potential models which reproduce the experimental phase shift data [25]. All these phenomenological potential models use OPE and OBE to explain the various properties of the interaction.

All these potential models had the following lacunae:

1. The existence of the scalar σ meson is controversial [1]. The scalar mesons have very large decay widths and thus the signal from the scalar mesons overlaps with those from the resonances and the background. These decay widths are further complicated by the presence of the $K\bar{K}$ and $\eta\eta$ decay channels in the vicinity of the scalar meson decays and due to the presence of the non- $q\bar{q}$ states like glue-balls.

2. These models were developed assuming the nucleons to be fundamental particles. But, the Deep Inelastic Scattering (DIS) experiments provided overwhelming evidence against the idea that nucleons were fundamental [26]. It was clear from the DIS experiments that the nucleons had a structure. The above potential models do not incorporate the structure of the nucleons.

1.3 Deep Inelastic Scattering (DIS)

The Deep Inelastic Scattering (DIS) experiments were a series of electron - proton scattering experiments conducted in the 1960's to study the structure of the nucleons. Electrons were scattered off of the protons at energies between 7 GeV and 17 GeV. The experiments measured the scattering cross section as a function of the angle of scattering. The results were compared with the cross sections for Rutherford and Mott scattering. Rutherford scattering corresponds to the elastic scattering of spinless point particles and the differential cross section is given by,

$$\frac{d\sigma_R}{d\omega} \propto \text{cosec}^4\left(\frac{\theta}{2}\right)$$

Mott scattering formula gives the differential cross section for the inelastic scattering of spin- $\frac{1}{2}$ point - particles

$$\frac{d\sigma_M}{d\omega} \propto \frac{1}{E^2} \text{cosec}^4\left(\frac{\theta}{2}\right) \cos^2\left(\frac{\theta}{2}\right)$$

Both the formulas above correspond to scattering of point particles. Thus if the nucleons were fundamental particles, the DIS cross section would have had a form similar to the Mott cross sections. But the DIS cross section deviated from it to a great extent and thus proved conclusively that the nucleons were not fundamental. Further, the differential cross section for the detection of the electrons gives the nucleon form factor as [27],

$$F(q) = G_2 + 2G_1 \tan^2\left(\frac{\theta}{2}\right)$$

where, G_2 and G_1 are the electric and magnetic form factors and the left hand side of the equation represents the ratio of the observed differential cross section to the Mott cross section. The ratio of the form factors, $\frac{G_2}{G_1}$, is in fact proportional to $\frac{Q^2}{\nu^2 + Q^2}$ where Q^2 is the momentum transfer and ν is the electron energy loss. Bjorken suggested [28] that the structure functions could depend on ν and Q^2 as

$$G_2 = \frac{1}{\nu} F_2(x)$$

where $x = \frac{2M\nu}{Q^2}$. This dependence of the structure functions on ratio of the energy loss to the momentum transfer is called the Bjorken scaling. Thus the function $F_2(x)$ is a universal function. This scaling behavior was *approximately* followed in the electron - proton scattering.

However, subsequent works showed that the none of the fields known at the time exhibited this behavior. In fact, it was proved that the theories violated Bjorken scaling order by order when perturbatively calculated. It was also shown that the Bjorken scaling is mildly violated in asymptotically free theories [29, 30, 31]. This gave credibility to Quantum Chromodynamics (QCD).

By the time DIS experiments were conducted, the accelerators around the world had found more than 40 types of hadrons nearly half of which were ground state particles and hence relatively stable. This posed a new puzzle: were all these particles fundamental? Was there a smaller set of particles which were fundamental and various combinations of which resulted in this zoo of hadrons?

1.4 Quantum Chromodynamics (QCD)

It was the work of Murray Gell-Mann [32, 33] and others [34, 35, 36] that resulted in a fundamental theory of the nucleons in particular and the hadrons in general called the Quantum Chromodynamics (QCD). Gell-Mann proposed that the nucleons - and all other hadrons - were made up of fundamental particles called quarks. The QCD Lagrangian is,

$$\mathcal{L}_{QCD} = \sum_f (\bar{\psi}_f i \gamma^\mu D_\mu \psi_f - m \bar{\psi}_f \psi) - \frac{1}{4} G_{\mu\nu}^a G^{\mu\nu a} \quad (1.1)$$

where, ψ_f is the quark field, the index f represents the flavour of the quarks, and $G_{\mu\nu}^a$ is the field strength tensor given by,

$$G_{\mu\nu}^a = \partial_\mu A_\nu^a - \partial_\nu A_\mu^a + g f^{abc} A_\mu^b A_\nu^c$$

The index a represents the color degrees of freedom.

The interaction between the quarks obeys $SU(3)_c$ local symmetry and the quarks possess, in addition to electric charge, color and flavor charges. The color charges came in three types - *red*, *green*, and *blue*. The quarks transform as triplets under this symmetry and all states that are physically observable can only transform as singlets. Thus, physically observable strongly interacting systems must be

color neutral. It is known that most of the mesons form the [36] representation and the baryons form the S - and P -waves form the [56] and [70] representations of the $SU(6)_q \times SU(6)_{\bar{q}}$ symmetry respectively.

The gluons, likewise, transform as the octets of $SU(3)_c$ local symmetry. The symmetry being exact implies that the gluons do not carry electric charges. An interesting consequence of the symmetry of QCD is that unlike the photons, gluons can interact with each other and form bound states because they are not color neutral.

In addition, QCD possesses the following properties:

1. QCD exhibits confinement:

$SU(3)$ color symmetry is a non-Abelian gauge symmetry obeyed by the quarks and gluons. This symmetry demands that *all physically observable states be color neutral states*. Thus one cannot observe free quarks in nature. This property is called confinement.

Confinement arises because of the nature of the interaction between colored particles. The energy of interaction shows an incremental behavior as the distance between two colored particles is increased. Thus, it is energetically impossible to separate two quarks or it is energetically favorable to create additional quark - anti - quark pairs as the distance between the quarks increases, thereby, preserving the color neutrality of the physically observable state.

2. QCD exhibits asymptotic freedom:

The QCD coupling constant falls off with energy. This makes the theory perturbative in the high energy regime. The scale one compares the energy regime with is the mass of the vector mesons. Since the lightest of the vector mesons are as light as $\sim 1\text{GeV}$, at all energies above this scale QCD of these quarks is perturbative. This property is called asymptotic freedom [37]. One should note that QCD is non - perturbative only at very low energies. Asymptotic freedom implies that the theory displays infrared slavery where, the strong coupling constant α_s decreases as the energy increases.

3. Being an asymptotically free theory, strongly interacting systems - bound states of colored particles - approximately follow Bjorken scaling. Thus the left hand side of the equation below is non - zero, which confirms the presence of Bjorken scaling in the system, where as, $F_2(x)$ is not strictly independent of Q^2 . Thus QCD follows Bjorken scaling only approximately.

$$\lim_{Q^2 \rightarrow \infty, \frac{\nu}{Q^2} \text{ fixed}} \nu G_2(x) = M F_2(x)$$

However, in spite of the knowledge of the existence of asymptotic freedom and confinement, these properties have not been explicitly included in the QCD Lagrangian. This is one of the most fundamental and unsolved problems of QCD. It is for this reason that all attempts at describing the properties of hadrons either involve free parameters or are effective theories.

1.5 QCD inspired Nuclear Models

The discussions of the previous section clearly imply that any attempt at explaining NN interaction must be rooted firmly in QCD. In this section, we review the various models of the nucleon inspired by QCD. The primary difference between these models and other phenomenological models is that the QCD inspired models use quarks and gluons as the fundamental degrees of freedom instead of the nucleons and mesons. These models use One - Gluon Exchange (OGE) for the short range and meson exchange for the intermediate and the long range interactions. The quark models - both relativistic and nonrelativistic - have been employed to study NN interaction.

Quark model becomes necessary even in case of meson exchange models. Since the charge radius of the nucleon and the theoretical rms radius of the mesons are almost identical (~ 0.6 fm), the structure of the mesons becomes important when discussing the meson exchange at scales less than ~ 2 fm. Thus, the short range interactions can only be described by QCD. It was shown by Shimizu and Yamazaki [38] that the $p\Sigma^+$ interaction potential is highly non-local. The non-locality arises only in the quark model calculations and thus can be attributed to the nucleon substructure. Hence the short range interaction cannot be explained using the conventional meson exchange potentials. Isgur and Maltman [39] studied the NN interaction using the OGE as the interacting potential. This study showed that the short range repulsion arises entirely due to the spin - spin interaction between the quarks.

All the QCD based quark models discussed above have a confining potential in addition to the interaction potential. The Hamiltonian is of the form,

$$H = \sum_i \left(\frac{p_i^2}{2m_i} \right) + \sum_{i < j} (V_{ij}^{conf} + V_{ij}^{int}) - E_{com}$$

where m_i and p_i are respectively the mass and the momentum of the i^{th} quark, V_{ij} are the potentials between the i^{th} and the j^{th} quarks and E_{com} is the center of mass energy. The center of mass energy can be subtracted by making a transformation to the Jacobi coordinates.

One assumes the ground state solution of the harmonic oscillator as the quark wave function and treats the interaction as a perturbation. The strong coupling

constant (α_s) of the interaction potential is treated as a parameter and so is the oscillator size. These models are all nonrelativistic quark models (NRQM) and they treat quarks as constituent particles with an effective mass $\sim 300\text{MeV}$.

Another class of the quark models are the so called bag models. These models tried to overcome the deficiency of the NRQM where quarks were treated as nonrelativistic particles. The quarks in addition to having a constituent mass of $\sim 300\text{MeV}$, because of the small volume of the nucleons, possess a momentum of the same order, there by making them relativistic. These relativistic effects are bundled into the coupling constants in the NRQM. But the bag models try to deal with the quarks in the relativistic way. One of the earliest and most successful bag model is the MIT bag model (for a good review see [40]). The bag models conjecture that the quarks and the gluons are confined to a “bubble” or a “bag”. These “bags” are tiny regions in the QCD vacuum. Since the quarks and the gluons possess large momenta inside these bags, they interact rather weakly with one another because of the asymptotic freedom of QCD. Thus, one can treat the interaction between the quarks in the bag perturbatively. The quarks and the gluons need to obey certain boundary conditions to preserve color neutrality of the baryons. However, the bag models lack translational invariance and exhibit spurious center of mass motion. Hence, the bag models are unsuitable for calculating the NN interaction. In addition to the above difficulties, the MIT bag model cannot explain the long range properties of the NN interaction.

The massless QCD Lagrangian possess chiral symmetry which is spontaneously broken. This spontaneous symmetry breaking leads to the creation of an octet of pseudoscalar Nambu - Goldstone bosons. These mesons constitute the partially conserved axial-vector current (PCAC) (for a review, see [41]). This symmetry breaking and the PCAC can be taken into account by including the OBE potentials. Since pion is the lightest of the mesons, the range of OPE is the largest among the OBEs. Since the short and intermediate range interactions cannot be described using OBEs, the only meson exchange one can include in NN interaction is the OPE for the long range part of the NN interaction.

Chapter 2

The Model

In the present work, we aim to calculate the adiabatic NN interaction potential for the singlet (1S_0) and the triplet (3S_1) states in the framework of the $SU(2)$ NRQM using RGM. The contributions of the kinetic energy of the quarks, the confinement potential and the various components of the interaction potentials are investigated. A comparison of these components of the Hamiltonian gives insights in to the behavior of the NN interaction and the physics underlying the interaction.

2.1 The Hamiltonian

The Hamiltonian used in the present work is,

$$H = K - K_{CM} + V_{OGEP} + V_{III} + V_{OPEP} + V_{CONF} \quad (2.1)$$

In the Hamiltonian, V_{OGEP} represents the OGEP, V_{III} represents the Instanton Induced Interaction, V_{OPEP} represents the OPEP, and V_{CONF} the confinement potential. The kinetic energies are,

$$K = \frac{1}{2m_q} \sum_{i=1}^6 p_i^2 \quad (2.2)$$

$$K_{CM} = \frac{1}{12m_q} P_{CM}^2 \quad (2.3)$$

The forms of the potentials are given below.

$$V_{OGEP} = \frac{\alpha_s}{4} \sum_{i < j} \left(\frac{1}{r_{ij}} - \frac{\pi}{m_q^2} \left(1 + \frac{2}{3} \boldsymbol{\sigma}_i \cdot \boldsymbol{\sigma}_j \right) \delta(\mathbf{r}_{ij}) \right) \boldsymbol{\lambda}_i \cdot \boldsymbol{\lambda}_j \quad (2.4)$$

$$V_{III} = - \sum_{i < j} \frac{1}{2} W_{ij} (1 - P_{ij}^f) \left[1 - \frac{1}{5} (\boldsymbol{\sigma}_i \cdot \boldsymbol{\sigma}_j) \right] \delta(\mathbf{r}_{ij}) \quad (2.5)$$

$$V_{OPEP} = \frac{f_Q^2}{3} \sum_{i < j} \frac{e^{-m_\pi r_{ij}}}{r_{ij}} (\boldsymbol{\sigma}_i \cdot \boldsymbol{\sigma}_j) (\boldsymbol{\tau}_i \cdot \boldsymbol{\tau}_j) \quad (2.6)$$

$$V_{CONF} = -a_c r_{ij}^2 \boldsymbol{\lambda}_i \cdot \boldsymbol{\lambda}_j \quad (2.7)$$

where the indices i and j run from 1 to 6. In the above expressions, r_i is the position of the i^{th} quark, $\boldsymbol{\sigma}_i$ is the spin of the i^{th} quark, $\boldsymbol{\tau}_i$ is the isospin of the i^{th} quark, $\boldsymbol{\lambda}_i$'s are the Gell-mann matrices, m_q is the mass of the quarks, m_π is the mass of the pion, α_s is the quark - gluon coupling constant, a_c is the confinement strength parameter, W_{ij} are the III coefficients, and $f_Q^2 = \frac{f_{\pi NN}^2}{4\pi}$ [42]. The number of III coefficients depends on the number of flavors of quarks in the model. In the $SU(2)$ NRQM, there are only two flavors of quarks and hence there is only one III coefficient W .

In the next section, we discuss the individual potentials.

2.2 One-Gluon Exchange Potential (OGEP)

Conventionally, NN interaction has been explained using meson exchange models. However, for the reasons explained in the previous chapter, it is imperative that the NN interaction models must be based on QCD. The QCD Lagrangian is given in 1.1.

The mechanism of one gluon exchange was proposed by Wilson [43], Kogut and Susskind [44] using the technique of lattice gauge theory. In lattice gauge theory, the quark fields are defined at lattice points and the gluon fields act as the links between the lattice points. The interaction energy can be expanded in the powers of $\frac{1}{\alpha_s}$ where α_s is the quark-gluon coupling constant. It was shown that this interaction energy increases with the lattice spacing and that the leading term in the expansion depends on the number of lattice point between the two quarks. Hence, the force between the quarks remains constant at large distances. Further, the spin-spin interaction decreases with increase in distance. Hence, the spin-spin interactions are short range forces or in other words, the short range behavior of the quark interaction must arise from spin-spin interactions [44]. These observations were used by de Rujula *et. al.* to derive the OGEP [45].

OGEP is derived from the tree level quark-quark interaction. In fact, it is the simplest possible interaction between the quarks. The Feynman diagram corresponding to one gluon exchange is given in fig.2.1

The amplitude for the above diagram is given by

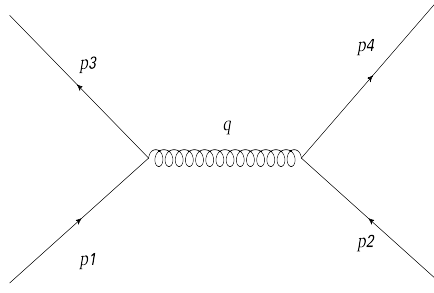


Figure 2.1: Tree level diagram for one gluon exchange.

$$\mathcal{M}_{fi} = g^2 \bar{u}(p_4) \gamma^\mu \frac{\lambda^a}{2} u(p_2) \left(g_{\mu\nu} + (\xi - 1) \frac{(p_3 - p_1)_\mu (p_3 - p_1)_\nu}{(p_3 - p_1)^2} \right) \bar{u}(p_3) \gamma^\mu \frac{\lambda^a}{2} u(p_1)$$

The bispinor amplitude u up to $\frac{1}{c^2}$ is given by

$$u(p) = \sqrt{2m} \begin{pmatrix} (1 - \frac{\mathbf{p}^2}{8m^2 c^2}) w(p) \\ (\frac{\boldsymbol{\sigma} \cdot \mathbf{p}}{2mc}) w(p) \end{pmatrix}$$

where w is the Schrödinger amplitude for the free particle. Using this in the expression for the amplitude, we get,

$$\mathcal{M}_{fi} = -2m_1 2m_2 (w^*(p_4) w^*(p_3) U(\mathbf{p}_1, \mathbf{p}_2, \mathbf{q}) w(p_2) w(p_1))$$

where,

$$U(\mathbf{p}_1, \mathbf{p}_2, \mathbf{q}) = \frac{g^2}{4\pi} \left\{ \frac{1}{\mathbf{q}^2} - \frac{1}{8m_1^2 c^2} - \frac{1}{8m_2^2 c^2} - \frac{(\boldsymbol{\sigma}_1 \cdot \boldsymbol{\sigma}_2)}{4m_1 m_2 c^2} + \frac{(\mathbf{q} \cdot \mathbf{p}_1)(\mathbf{q} \cdot \mathbf{p}_2)}{m_1 m_2 \mathbf{q}^2} - \frac{(\mathbf{p}_1 \cdot \mathbf{p}_2)}{m_1 m_2 \mathbf{q}^2} + \dots \right\} \frac{\boldsymbol{\lambda}_1 \cdot \boldsymbol{\lambda}_2}{4} \quad (2.8)$$

This represents the one gluon exchange potential in the momentum space. Taking the Fourier transform of the above equation gives the OGEP between two quarks in the coordinate space. The central and the color magnetic part of the OGEP is given by eq. (2.4). We see that $\alpha_s = \frac{g^2}{4\pi}$. The details of this derivation in the Breit frame can be found in [46]

The Coulomb-like part of the OGEP gives the long range behavior of quark - quark interactions and is independent of the quark masses and spins as the phenomenon of confinement is observed across all quark flavors. But, the color magnetic and color electric interactions depend on quark mass. These forces are short

range forces and arise from one gluon exchange. The color magnetic interaction also provides the hyperfine splitting of the hadron masses.

However, the OGEP does not take into account the spontaneous symmetry breaking of the QCD Lagrangian. The dynamical breaking of the chiral symmetry in the OGEP model is due to the finite mass of quarks and the OGEP does not provide an explanation for the existence of the pseudoscalar mesons and hence is incomplete.

2.3 Instanton Induced Interaction (III)

Consider the case of massless free quarks. The Lagrangian is given by,

$$\mathcal{L}_{massless}^{free} = \sum_f (\bar{\psi}_f i\gamma^\mu \partial_\mu \psi_f) \quad (2.9)$$

The Lagrangian possesses the global $SU(N_f) \times U(1)$ symmetry. The quark spinors ψ can be decomposed in to $\psi = \psi_L + \psi_R$. Upon substituting this decomposition, the Lagrangian above reduces to (the flavor index f is suppressed and the summation over f is implied)

$$\mathcal{L}_{massless}^{free} = \bar{\psi}_L i\gamma^\mu \partial_\mu \psi_L + \bar{\psi}_R i\gamma^\mu \partial_\mu \psi_R \quad (2.10)$$

The decomposition of the bispinor in to ψ_L and ψ_R can be achieved using the projection operators $P_L = \frac{1}{2}(1 - \gamma_5)$ and $P_R = \frac{1}{2}(1 + \gamma_5)$.

$$P_L \psi = \frac{1}{2}(1 - \gamma_5)\psi = \psi_L, \quad P_R \psi = \frac{1}{2}(1 + \gamma_5)\psi = \psi_R$$

The Lagrangian in eq.2.9 possesses $SU(N_f)_V \times SU(N_f)_A \times U(1)_V \times U(1)_A$ symmetry - it can be decomposed completely in to the “left” and the “right” components as shown in eq. 2.10. However, the Lagrangian (eq.2.9) describes massless free quarks. The introduction of mass into eq.2.9 destroys the chiral symmetry as the mass terms gives rise to the mixing of the “left” and “right” components of the quark field. The presence of mass of the quarks breaks the chiral symmetry dynamically.

It was shown that the chiral symmetry is broken not only dynamically by the non-zero mass of the quarks but also spontaneously [47, 48]. The $U(1)_A$ symmetry shows anomalous behavior and the corresponding axial vector current j_μ^5 is not conserved. This spontaneous symmetry breaking leads to the existence of Nambu-Goldstone pseudoscalar mesons in the theory. These mesons in the QCD are massive because the constituent quarks are massive. The spontaneous breaking of chiral symmetry is believed to be due to instantons [49].

Instantons are a class of pseudo-particles which form the solutions to the QCD Lagrangian in the asymptotic limit. Instanton fields satisfy the equation of motion $D_\mu^{ab} F^{\mu\nu b} = 0$ in the Euclidean space. They also serve as a mechanism for chiral symmetry breaking, which results in the light quarks acquiring a dynamical mass [50, 51]. This results in the mass of any physically observable system made up of light quarks being much greater than the sum of the current masses of the constituent quarks. This can also be thought of as the quarks acquiring dynamical mass due to III. Thus the III play a major role in the properties of light hadrons and their interactions.

The instanton solutions were first proposed by Belavin *et. al.* in 1975 [52]. The properties of instantons and their influence on hadron spectra were studied extensively by Kochelev [51] and Shuryak [50]. The influence of III on NN interaction was first studied by Oka and Takeuchi [53]. The III potential they used had the form

$$V_{III} = - \sum_{i < j} W_{ij} (1 - P_{ij}^f) \left[1 - \frac{1}{5} \boldsymbol{\sigma}_i \cdot \boldsymbol{\sigma}_j \right] \delta(\mathbf{r}_{ij}) \quad (2.11)$$

where, P_{ij}^f denotes flavor exchange. Evidently, III exists only between those quark pairs which are antisymmetric under flavor exchange. The flavor exchange operation is equivalent to color and spin exchange and hence can be written as $P_{ij}^f = -P_{ij}^s P_{ij}^c$. The coefficient W_{ij} is related to the quark condensate and is inversely proportional to the product of the masses of the interacting quarks. In the $SU(2)$ NRQM, the potential is given by

$$V_{III} = -\frac{W}{2} \sum_{i < j} \left(\frac{16}{15} + \frac{2}{5} \boldsymbol{\lambda}_i \cdot \boldsymbol{\lambda}_j + \frac{1}{10} \boldsymbol{\sigma}_i \cdot \boldsymbol{\sigma}_j \boldsymbol{\lambda}_i \cdot \boldsymbol{\lambda}_j \right) \delta(\mathbf{r}_{ij}) \quad (2.12)$$

The color magnetic part leads to the hyperfine splitting of the baryon and meson spectra. The III also overcomes another drawback of the OGEP. With OGEP as the quark-quark interaction potential, faithful reproduction of the hyperfine splitting of the baryon spectra demands that the quark coupling constant $\alpha_s \sim 1.6$ [53]. This would make the perturbative expansion of the quark-quark interaction in terms of α_s divergent and hence invalid. Also, lattice QCD simulations show that the predicted values for hyperfine splitting in the quenched approximation are only half of the observed values [54]. These problems can be overcome by using III. Since III also contains color magnetic terms which will contribute to hyperfine splitting, the value of α_s can be reduced to half the original value, thereby rendering the perturbative expansion convergent, if we assume that the color magnetic terms of the OGEP and the III contribute equally to the mass splittings. Also, the color magnetic terms of the III will ensure that the mass splittings are of correct magnitude.

2.4 One-Pion Exchange Potential (OPEP)

The divergence of the axial vector current corresponding to the $SU(3)_A$ symmetry is proportional to the quark masses. In the limit of vanishing quark masses, $SU(N_f)_A$ transformations form a symmetry of the quark Lagrangian. Thus, these currents are called Partially Conserved Axial-vector Currents (PCAC). As discussed above, the chiral symmetry breaking leads to presence of pseudo-scalar Nambu-Goldstone mesons and the PCACs are nothing but these mesonic currents. In the present model, we consider the $SU(2)$ quarks only and hence, the only possible PCACs are the pion currents. Thus, from the symmetry breaking perspective, it is important that the model contains interactions between nucleons mediated by pions. It has also been shown in numerous models earlier that the long range behavior of the NN interaction is satisfactorily explained by the potential arising due to the exchange of one pion (for example [55]).

However, one cannot consider the pions in the model as $q\bar{q}$ pairs for the following reasons:

- Pair production and annihilation is not allowed in a nonrelativistic theory. Since the model is nonrelativistic, production of $q\bar{q}$ pairs i.e., pions cannot be justified. However, it is possible to derive the interaction potential of one pion exchange if one considers the pions to be fundamental fields which couple to the quarks.
- The $\pi - N$ coupling constant $f_{\pi NN}$ derived from NN scattering data does not match the values calculated from the models if the pions used in the model are treated as $q\bar{q}$ pairs. In fact the observed value of the coupling constant is nearly thrice that predicted by the model. If the value for $f_{\pi NN}$ is fitted into the model, then the mean square radius $\langle r^2 \rangle$ of the nucleon from the model turns out to be very large. Thus one cannot match both $f_{\pi NN}$ and $\langle r^2 \rangle$ simultaneously in a model that assumes pions to be $q\bar{q}$ pairs.

For the reasons described above, it is absolutely essential to include OPEP in the model and to treat the pions as fundamental fields [56]. This also enables us to treat pions as point particles and thereby eliminate a cut off parameter that has to be introduced otherwise. The form of the OPEP is given in eq.2.6. The potential has two parameters in the form of pion mass m_π and the coupling constant f_Q^2 . The later is related to $f_{\pi NN}$ via the Goldberger-Treiman relation $f_Q^2 = \frac{f_{\pi NN}^2}{4\pi}$ [42].

2.5 Resonating Group Method (RGM)

In this section, we discuss the method used to evaluate the Hamiltonian matrix elements. We use RGM developed by Wheeler in the year 1937 [57] (for reviews of NN interaction using RGM see [58, 59]). For the sake of evaluation we designate the two nucleons as A and B . We further label the quarks belonging to nucleon A as 1, 2, and 3 and those belonging to nucleon B as 4, 5, and 6. We begin by constructing the single nucleon wave function.

2.5.1 Wave function of a Nucleon

The nucleon has orbital (O), spin (S), isospin (T), and color (C) degrees of freedom. Since nucleons are fermions, their wave functions must be antisymmetric. The color wave function is a totally antisymmetric wave function because the nucleon is a color singlet. In the NRQM study of the NN interaction, the interaction potentials V_{OGEP} , V_{III} and V_{OPEP} are considered to be perturbations acting on the system of quarks moving in the harmonic oscillator like confinement potential. Thus in the ground state, the orbital part of the quark wave function is given by

$$\phi(\mathbf{r}_i) = \frac{1}{(\pi b^2)^{3/4}} \exp\left(-\frac{1}{2b^2}(\mathbf{r}_i)^2\right)$$

where b is the oscillator size parameter, and \mathbf{r}_i is the position of the i^{th} quark. The ground state is characterized by zero angular momentum, ($l = 0$) and even parity. Thus the orbital wave function of the three quark ground state is

$$\phi(\mathbf{r}_i) = \frac{1}{(\pi b^2)^{9/4}} \prod_{i=1}^3 \exp\left(-\frac{1}{2b^2}(\mathbf{r}_i)^2\right) \quad (2.13)$$

This wave function is symmetric under the exchange of quarks.

In the $SU(2)$ NRQM, the spin - isospin symmetry of the the multi quark state is defined by the irreducible representations of the $SU(2)_{spin} \times SU(2)_{isospin}$ group. Since each quark is a spin- $\frac{1}{2}$ and isospin- $\frac{1}{2}$ particle, the nucleon spin and isospin wave functions can only be either mixed symmetric or mixed antisymmetric. The mixed symmetric (MS) wave functions of a proton are

$$\phi_{MS}^{spin} = \frac{1}{\sqrt{6}}[(\uparrow\downarrow + \downarrow\uparrow)\uparrow - 2\uparrow\uparrow\downarrow] \quad (2.14)$$

$$\phi_{MS}^{isospin} = \frac{1}{\sqrt{6}}[(ud + du)u - 2uud] \quad (2.15)$$

The corresponding mixed antisymmetric (MA) wave functions are,

$$\phi_{MA}^{spin} = \frac{1}{\sqrt{2}}(\uparrow\downarrow - \downarrow\uparrow) \uparrow \quad (2.16)$$

$$\phi_{MA}^{isospin} = \frac{1}{\sqrt{2}}(ud - du)u \quad (2.17)$$

Thus the spin-isospin wave function of the proton is

$$|P\rangle = \frac{1}{\sqrt{2}}[\phi_{MS}^{spin} \phi_{MS}^{isospin} + \phi_{MA}^{spin} \phi_{MA}^{isospin}]$$

Hence, the spin-isospin wave function of a nucleon is symmetric under the exchange of quarks.

The color wave function of a nucleon is given by,

$$\frac{1}{\sqrt{6}}[RGB - RBG + BRG - BGR + GBR - GRB]$$

where, R, G, and B represent the three colors - red, green, and blue respectively. One can easily note that the color wave function is totally antisymmetric under the exchange of two quarks. Thus the total wave function of a single nucleon has the form,

$$\psi = \boxed{1}\boxed{2}\boxed{3}^O \otimes \frac{1}{\sqrt{2}} \left[\boxed{1}\boxed{2}^S \boxed{3}_{MS}^T \oplus \boxed{1}\boxed{2}^S \boxed{3}_{MA}^T \right] \otimes \boxed{1}^C \boxed{2} \boxed{3}$$

2.5.2 Wave function of a two Nucleon system

To construct the eigenfunction of a two nucleon system we look at its symmetries. Each nucleon is made up of three quarks in their ground state and hence each nucleon belongs to the [3] representation of the orbital symmetry. Thus the orbital symmetry of the two nucleon system is

$$[3] \otimes [3] = [6] \oplus [42] \oplus [51] \oplus [33]$$

$$\begin{array}{|c|c|c|} \hline & & \\ \hline \end{array} \otimes \begin{array}{|c|c|c|} \hline & & \\ \hline \end{array} = \begin{array}{|c|c|c|c|c|c|} \hline & & & & & \\ \hline \end{array} \oplus \begin{array}{|c|c|c|c|} \hline & & & \\ \hline & & & \\ \hline \end{array} \oplus \begin{array}{|c|c|c|c|c|c|} \hline & & & & & \\ \hline & & & & & \\ \hline & & & & & \\ \hline \end{array} \oplus \begin{array}{|c|c|c|} \hline & & \\ \hline & & \\ \hline & & \\ \hline \end{array}$$

The ST wave function also possesses the symmetry mentioned above. The color wave function is totally antisymmetric and hence the two nucleon color wave function has the following symmetry

$$\begin{array}{|c|} \hline \\ \hline \\ \hline \\ \hline \end{array} \otimes \begin{array}{|c|} \hline \\ \hline \\ \hline \\ \hline \end{array} = \begin{array}{|c|c|} \hline & \\ \hline & \\ \hline & \\ \hline & \\ \hline \end{array} = [222]$$

Since each nucleon has a totally antisymmetric color wave function, the product of the two wave functions does not necessarily yield a totally antisymmetric state. Imposing this condition on the two nucleon state makes the wave functions with the following symmetries are admissible for a two nucleon system:

1. $[6]_O \otimes [33]_{ST} \otimes [222]_c$
2. $[42]_O \otimes [51]_{ST} \otimes [222]_c$
3. $[42]_O \otimes [33]_{ST} \otimes [222]_c$

Hence the totally antisymmetric wave function describing a two nucleon system is

$$\psi_{TOT} = \psi^c[a[6]^O[33]^{ST} + b[42]^O[51]^{ST} + c[42]^o[33]^{ST}]$$

where the superscripts O , ST , and c imply orbital, spin-isospin, and color respectively. The coefficients a , b , and c are the Clebsch-Gordon coefficients. With this setup, we move on to discuss the RGM for a two nucleon system.

In the RGM formalism, nucleons are considered as clusters of 3 quarks. Thus a two nucleon system is treated as a system of two clusters with 3 quarks each. The two nucleon wave function is nothing but the product of the wave functions of each nucleon. The interaction between the nucleons arises because of the exchange of quarks between the clusters. The exchange of quarks is possible only if the wave functions of the two nucleons overlap. The wave function of the two nucleon system when the nucleons are well separated is given by

$$\psi = \mathcal{A}[\phi_A \phi_B \chi] \quad (2.18)$$

where, the clusters are named A and B and ϕ_A and ϕ_B are their wave functions respectively. χ is the relative wave function. \mathcal{A} is the anti-symmetrization operator. The orbital part of the wave function is given by

$$\begin{aligned} \phi(\mathbf{r}_A) &= \frac{1}{(\pi b^2)^{9/4}} \prod_{i=1}^3 \exp\left(-\frac{1}{2b^2}\left(\mathbf{r}_i - \frac{\mathbf{s}_I}{2}\right)^2\right) \\ \phi(\mathbf{r}_B) &= \frac{1}{(\pi b^2)^{9/4}} \prod_{i=4}^6 \exp\left(-\frac{1}{2b^2}\left(\mathbf{r}_i + \frac{\mathbf{s}_I}{2}\right)^2\right) \end{aligned}$$

where \mathbf{s}_I is the generator coordinate. The difference in the sign of the generator coordinates of the two clusters implies that the clusters are separated by a distance \mathbf{s}_I . To write the total wave function ψ in the above form, we employ the following transformations.

$$\begin{aligned}
\boldsymbol{\xi}_1 &= \mathbf{r}_1 - \mathbf{r}_2, & \boldsymbol{\xi}_2 &= \mathbf{r}_3 - \frac{\mathbf{r}_1 + \mathbf{r}_2}{2}, & \mathbf{R}_A &= \frac{1}{3}(\mathbf{r}_1 + \mathbf{r}_2 + \mathbf{r}_3) \\
\boldsymbol{\xi}_3 &= \mathbf{r}_4 - \mathbf{r}_5, & \boldsymbol{\xi}_4 &= \mathbf{r}_6 - \frac{\mathbf{r}_4 + \mathbf{r}_5}{2}, & \mathbf{R}_B &= \frac{1}{3}(\mathbf{r}_4 + \mathbf{r}_5 + \mathbf{r}_6) \\
\mathbf{R}_{AB} &= \mathbf{R}_A - \mathbf{R}_B, & \mathbf{R}_G &= \frac{1}{2}(\mathbf{R}_A + \mathbf{R}_B)
\end{aligned}$$

Here, \mathbf{r}_i gives the position of the i^{th} quark; $\boldsymbol{\xi}_i, i = 1, 2(3, 4)$ are the internal coordinates of the cluster A(B) respectively. \mathbf{R}_{AB} is the relative coordinate and \mathbf{R}_G is the coordinate of the center of mass of the system. From this we can write the RGM wave function as

$$\psi(\boldsymbol{\xi}_1, \boldsymbol{\xi}_2, \boldsymbol{\xi}_3, \boldsymbol{\xi}_4, \mathbf{R}_{AB}) = \mathcal{A}[\phi_A(\boldsymbol{\xi}_1, \boldsymbol{\xi}_2)\phi_B(\boldsymbol{\xi}_3, \boldsymbol{\xi}_4)\chi(\mathbf{R}_{AB})]$$

where, ϕ_A and ϕ_B are the internal wave functions of the two clusters and χ is the relative wave function. The anti-symmetrization operator is given by

$$\mathcal{A} = 1 - \sum_{i \in A, j \in B} P_{ij}^{OSTC}$$

The following arguments are to be kept in mind while constructing the operator. When the nucleons are sufficiently close, their wave functions overlap to a considerable extent. When this happens, any one or more quarks belonging to one nucleon can be exchanged with an equal number of quarks of the other nucleon. Three quark exchange results in the interchange of the nucleons themselves; two quarks exchange can be thought of as one quark exchange plus an interchange of nucleons. Thus only one quark exchanges matter. Since quarks are identical indistinguishable particles, only the number of quarks exchanged needs to be considered and there are 9 ways of exchanging one pair of quarks between two nucleons. Thus the anti-symmetrization operator is

$$\mathcal{A} = \frac{1}{10}(1 - 9P_{36}^{OSTC}) \quad (2.19)$$

where the operator P_{36}^{OSTC} exchanges the orbital, spin, isospin and color quantum numbers of the quarks 3 and 6.

To calculate the NN potential, one finds the solution to the equation

$$\langle \psi | (H - E) \mathcal{A} | \psi \rangle = 0$$

The following kernels can be calculated from the above equation:

1. Normalization kernel: $N = \langle \psi | \mathcal{A} | \psi \rangle$
2. Kinetic energy kernel: $K = \langle \psi | (K - K_{CM}) \mathcal{A} | \psi \rangle$, and

3. Potential energy kernel: $V = \langle \psi | (V_{Int} + V_{Conf}) \mathcal{A} | \psi \rangle$

where, V_{Int} represents the interaction potential between the quarks. Thus the energy of the interaction is given by

$$E = \frac{\langle \psi | H \mathcal{A} | \psi \rangle_l}{\langle \psi | \mathcal{A} | \psi \rangle_l}$$

where the subscript l implies that the matrix elements have been projected to the angular momentum channel l . In terms of the kernels,

$$E = \frac{(K + V)_l}{N_l}$$

In terms of the internal and relative coordinates, the above equations can be rewritten as

$$\begin{aligned} \mathcal{L}_{IJ}^l = & \int [\phi_A^+(\boldsymbol{\xi}_A) \phi_B^+(\boldsymbol{\xi}_B) \frac{\chi_I^l(\mathbf{R}_{AB})}{\mathbf{R}_{AB}} Y_{lm}^*(\hat{\mathbf{R}}_{AB})] \phi(\mathbf{R}_G) (H - E) \otimes \\ & \mathcal{A} [\phi_A(\boldsymbol{\xi}_A) \phi_B(\boldsymbol{\xi}_B) \frac{\chi_I^l(\mathbf{R}_{AB})}{\mathbf{R}_{AB}} Y_{lm}(\hat{\mathbf{R}}_{AB})] \phi(\mathbf{R}_G) d\mathbf{R}_G d\mathbf{R}_{AB} d\boldsymbol{\xi}_A d\boldsymbol{\xi}_B \end{aligned}$$

where $\boldsymbol{\xi}_A$ and $\boldsymbol{\xi}_B$ represent the internal coordinates of the two clusters. In the quark coordinates, the above equation can be written as

$$\begin{aligned} \mathcal{L}_{IJ}^l = & \int [\phi_A^+(\mathbf{r}_1, \mathbf{r}_2, \mathbf{r}_3; \frac{\mathbf{s}_I}{2}) \phi_B^+(\mathbf{r}_4, \mathbf{r}_5, \mathbf{r}_6; \frac{-\mathbf{s}_I}{2}) Y_{lm}^*(\hat{\mathbf{S}}_I)] (H - E) \otimes \\ & \mathcal{A} [\phi_A(\mathbf{r}_1, \mathbf{r}_2, \mathbf{r}_3; \frac{\mathbf{s}_I}{2}) \phi_B(\mathbf{r}_4, \mathbf{r}_5, \mathbf{r}_6; \frac{-\mathbf{s}_I}{2}) Y_{lm}(\hat{\mathbf{S}}_I)] \prod_{k=1}^6 d^3\mathbf{r}_k d\hat{\mathbf{S}}_I d\hat{\mathbf{S}}_J \end{aligned} \quad (2.20)$$

The presence of the anti-symmetrization operator \mathcal{A} splits the Hamiltonian in to two - direct and exchange. The direct part of the Hamiltonian is $\langle \psi | \frac{1}{10} H | \psi \rangle_l$ and the exchange part is given by $\langle \psi | \frac{9}{10} H P_{36}^{QSTC} | \psi \rangle_l$. The direct part of the Hamiltonian has the following components: the kinetic energy of the individual quarks, the kinetic energy of the center of mass of the system, and the potential energy of the interaction between the quarks belonging to the same cluster. The inter-cluster direct interactions vanish because of the vanishing color interactions as per the Wigner - Eckart theorem. On the other hand, the exchange part of the Hamiltonian involves, in addition to the components mentioned above, inter-cluster interactions also. It is the exchange part of the Hamiltonian that gives rise to the NN interaction potential. The various components of the exchange part of the potential kernel are: V_{12}^{EX} , V_{13}^{EX} , V_{14}^{EX} , V_{16}^{EX} , and V_{36}^{EX} . The rest of the components of the interaction are equal to one of the components mentioned above. For example, V_{12}^{EX} is the same as V_{45}^{EX} , V_{14}^{EX} is the same as V_{15}^{EX} , V_{24}^{EX} , and

V_{25}^{EX} . Thus the components of the potentials add up as $2V_{12}^{EX} + 4V_{13}^{EX} + 4V_{14}^{EX} + 4V_{16}^{EX} + V_{36}^{EX}$. One can notice that there are 15 possible exchange components. The direct part of the potential kernel has only two unique components: V_{12}^D and V_{36}^D of which the latter vanishes. Since there can be 6 components of the former type, V_{12}^D is multiplied by a factor of 6. The exchange part of the kinetic energy has two types of components: K_1^{EX} and K_3^{EX} . There are two components of the latter type and 4 components of the former type. Thus the exchange part of the kinetic energy kernel is $4K_1^{EX} + 2K_3^{EX}$. The direct part has a similar structure. The various components of the different kernels are listed in the appendix A.1.3.

Since the quarks are lighter than the nucleons themselves, their kinetic energy is much greater than that of the nucleons. Thus the kinetic energy of the nucleons does not contribute to the NN interaction. To remove this component from the Hamiltonian, we use the Born - Oppenheimer approximation [60]. The exchange interactions lead to the NN potential. In the asymptotic limit of $\mathbf{s}_I \rightarrow \infty$, the Hamiltonian mentioned above gives the kinetic energies of the nucleons and their masses. The exchange part of the interactions vanish in this limit as the overlap between the wave functions is minimal. Thus, we subtract the total energy in the asymptotic limit from the total energy to obtain the NN interaction potential. This procedure is called the adiabatic approximation.

Chapter 3

Results and Discussion

In this chapter, we discuss in detail the results of the present work.

3.1 Hamiltonian and the Matrix elements

The Hamiltonian used in the present calculation is given in eq.(2.1). The total energy of the NN system has the direct and exchange parts of the following components:

1. Kinetic energy of quarks,
2. Coulomb part of the OGEP,
3. Color electric part of the OGEP,
4. Color magnetic part of the OGEP,
5. Confinement part,
6. Color electric part of III,
7. Color magnetic part of III,
8. Color independent part of III, and
9. One pion exchange potential.

To analyze the contributions of the various components of the Hamiltonian, we have plotted the diagonal elements of the various kernels of the singlet and triplet NN potentials as a function of the relative distance between the nucleons (s_I).

The adiabatic potential is calculated using the Born - Oppenheimer approximation given by,

$$V_{12}^{Ad} = \langle \psi_1(\mathbf{s}_I) | H | \psi_2(\mathbf{s}_I) \rangle - \langle \psi_1(\infty) | H | \psi_2(\infty) \rangle \quad (3.1)$$

where H is the Hamiltonian (eq.2.1) and $\psi_i(\mathbf{s}_I)$ is the normalized two nucleon wave function in the state i .

The contribution of the kinetic energy of the quarks to NN interaction is given in fig.B.1. Figs.B.2 and B.3 give the direct and the exchange part of the kinetic energy kernel respectively. The kinetic energy of quarks provides a state independent repulsion in the short range. Both the direct and the exchange components of the kinetic energy are repulsive in the short range. We note that the total kinetic energy of the quarks in the long range is approximately 160 MeV which is in the same range as the mass of the quarks which is ~ 300 MeV. This is in agreement with the previous results.

The contribution of the Coulombic part of the OGEP is given in fig.B.4 and its direct and exchange components in fig.B.5 and fig.B.6 respectively. The direct part of the interaction is attractive and the exchange part is repulsive. The net contribution is state independent attraction in the short range. We note that the depth of the attractive part is < 1 MeV. The color electric part of OGEP is plotted in fig.B.7 and its direct and exchange components in fig.B.8 and fig.B.9 respectively. The direct part of the interaction is repulsive and the exchange part is attractive in the short range. The net contribution is independent attraction in the short range. The contributions of the color magnetic part of OGEP is plotted in fig.B.10. The corresponding direct and exchange components are plotted in figs.B.11 and B.12 respectively. The direct part of the color magnetic part of OGEP gives a state independent attraction in the short range. The exchange part of the color magnetic interaction is repulsive and distinguishes between the singlet and triplet states. We note that the height of the repulsion is lesser for the triplet state (~ 45 MeV) than for the singlet state (~ 70 MeV). The distinction between the singlet and the triplet states arises from the spin-spin interaction present in the color magnetic part of the OGEP.

The III potential consists of three components - color independent part, color electric part, and the color magnetic part. The color independent part of the III is plotted in fig.B.13. Fig.B.14 and fig.B.15 give the plots of the direct and the exchange parts of the color independent part of III. The contribution of the color independent part of the III is attractive in the short range. Both the direct and the exchange parts are attractive. The color electric part of III is plotted in fig.B.16 and its direct and exchange components in fig.B.17 and fig.B.18 respectively. This part of III provides state independent attraction in the short range. The direct part is marginally repulsive (~ 0.3 MeV) in the short range whereas the exchange part is attractive. The contributions of the color magnetic part of III is plotted

in fig.B.19. The corresponding direct and exchange components are plotted in figs.B.20 and B.21 respectively. The direct part of the color magnetic part of III gives a state independent attraction in the short range. The exchange part of the color magnetic interaction is repulsive and distinguishes between the singlet and triplet states. We note that the height of the repulsion is lesser for the triplet state (~ 3 MeV) than for the singlet state (~ 6 MeV). We also note that the height of repulsion for both the singlet and the triplet states are nearly an order of magnitude lesser compared to the corresponding contribution from the OGEP.

The total contributions of OGEP and III are plotted in fig.B.22 and fig.B.23 respectively. Both the potentials distinguish between the singlet and the triplet states as both of them contain color magnetic interactions. The contribution of OGEP for the NN interaction is repulsive in the short range. This repulsion arises solely from the color magnetic interactions. Contrastingly, the contribution of III to the NN interaction is attractive in the short range. This attraction arises primarily due to the color independent interaction (first term in eq.2.12). We also note that the depth of attraction from III for the singlet state is smaller than the height of repulsion from OGEP whereas the depth of attraction for the triplet state is larger than the height of repulsion. Thus the combined contribution of the OGEP and the III for the singlet state is repulsive whereas that for the triplet state it is attractive.

The contributions of the OPEP is plotted in fig.B.24. The corresponding direct and exchange components are plotted in figs.B.25 and B.26 respectively. Both the direct and the exchange part of the OPEP give rise to state independent repulsion in the short range. The total contribution of the OPEP, hence, is repulsive in the short range.

The contributions of the confinement potential is plotted in fig.B.27. The corresponding direct and exchange components are plotted in figs.B.28 and B.29 respectively. The direct part of the confinement potential gives a small repulsion (< 1 MeV) in the short range but the exchange part of the potential dominates with a short range attraction.

The direct and exchange parts of the Hamiltonian are plotted in fig.B.30. The direct part provides a state independent attraction in the short and intermediate ranges. The exchange part distinguishes between the singlet and the triplet states and is repulsive for the singlet state and shows a small amount of attraction in the intermediate range for the triplet state. The direct part of the Hamiltonian corresponds to the self energy of the nucleons and hence is state independent. Since the exchange part of the Hamiltonian represents the interaction between the nucleons, the distinction between the singlet and the triplet states must arise from the exchange terms of the Hamiltonian. In fact, the distinction between the singlet and triplet states arises from the exchange part of the color magnetic terms of the

OGEP and III (fig.B.10 and fig.B.19).

The adiabatic potential for singlet and triplet states with and without OPEP are plotted in fig.B.31 and fig.B.32 respectively. In the absence of OPEP, the singlet potential exhibits a short range repulsion and an intermediate range attraction. The intermediate range attraction in the singlet state is removed when OPEP is introduced. The depth of attraction for the triplet potential decreases with the introduction of the OPEP. This is because the OPEP provides state independent repulsion in the short and the intermediate range (fig.B.24). One can also note that in the presence of OPEP, the short range repulsion is increased in both the singlet and the triplet states.

3.1.1 Parameters

The model has 7 parameters - oscillator size parameter (b), strong coupling constant (α_s), instanton induced interaction strength (W), mass of the quarks (m_q), confinement strength parameter (a_c), mass of the pion (m_π), and the OPEP strength parameter (f_Q). The values of these parameters have been chosen in the following way:

1. Strong coupling constant (α_s) and III parameter (W): The color magnetic parts of both OGEP and III contribute to the hyperfine splitting of the baryon mass. In the $SU(2)$ NRQM, nucleons and the Δ -resonances are the only allowed baryons in the $l = 0$ channel. These two particles differ only in their spin. The nucleons are spin- $\frac{1}{2}$ particles where as Δ are spin- $\frac{3}{2}$ particles. Hence the difference between their masses must arise purely out of the spin-spin interactions. Thus, if we assume that the color magnetic forces of OGEP and III contribute equally to the $N - \Delta$ mass splitting, we arrive at the following expressions for α_s and W using the single nucleon wave functions given in eq.2.13

$$\alpha_s = \frac{3m_q^2 b^3}{\sqrt{8\pi}} \left(\frac{\Delta m}{2} \right) \quad (3.2)$$

$$W = \frac{5b^3}{3\sqrt{2\pi}} \left(\frac{\Delta m}{2} \right) \quad (3.3)$$

where, Δm is the $N - \Delta$ mass difference.

2. Mass of the quark (m_q): As discussed in the previous chapter, the dynamical breaking of the chiral symmetry of the QCD Lagrangian results in the quarks acquiring a constituent mass. The electric and magnetic moments of the *up* and the *down* quarks gives an estimate of the constituent mass as ~ 330 MeV [61, 62]. In the present model, we have used the mass of the quarks as

a free parameter. It should be noted that the strong coupling constant α_s is sensitive to the value of the m_q . The strong coupling constant increases as the square of the mass of the quarks (eq.3.2). Also of importance is the observation that W does not depend on the mass of the quarks even though the quarks acquire the constituent mass due to the coupling with the instanton vacuum.

3. Oscillator size parameter (b): The oscillator size parameter is related to the r.m.s. radius of the nucleon as $\sqrt{r^2} = b$. NN scattering data suggest that the r.m.s value of the radius of the proton is close to 0.6 fm. We observe immediately that both α_s and W depend on the third power of b .

The values of the parameters used are tabulated below.

b (fm)	α_s	W (MeV fm^3)	a_c (MeV fm^{-2})	m_q (MeV)	m_π (MeV)	f_q^2
0.6	0.713	67.67	40.5	300.0	140.0	12.6

Table 3.1: List of parameters

Chapter 4

Summary and Conclusions

In this section we summarize the model described in the previous sections and the results obtained.

4.1 Summary of the work

We have constructed an $SU(2)$ nonrelativistic quark model to explain the central part of the NN interaction in the $l = 0$ state. The Hamiltonian consists of the kinetic energy of the quarks, a harmonic oscillator like confinement potential and the quark-quark interaction potentials. The quark-quark interaction potential include one-gluon exchange potential, instanton induced interaction potential and the one-pion exchange potential.

We have used the RGM to calculate the NN interaction potential. We find that the NN potential derived from this model follows qualitatively the potential derived from the NN scattering data. The NN potential derived from our model exhibits a short range repulsion, intermediate range attraction and long range saturation behavior. The model distinguishes between the spin singlet and triplet states in the short and intermediate ranges.

The interaction potentials form the perturbative interactions of the 6 quark NN system described by the kinetic energy and the harmonic confining potential. Hence, we have chosen the orbital part of the trial wave function as the ground state wave function of a harmonic oscillator. The spin, isospin and color wave functions have been constructed from the symmetry of the NN system. The interaction between the nucleons takes place because of the exchange of the quarks between the nucleons. To incorporate the fermionic nature of the NN system, we have constructed a suitable anti symmetrization operator.

The OGE consists of a Coulombic term, a color electric term and a color magnetic term. The III contains a color independent term, a color electric term and

a color magnetic term. The OPEP consists of the central Yukawa-like potential. The short range repulsion is provided by the kinetic energy of the quarks and the color magnetic part of the OGEP and the III. The color magnetic interactions between the quarks differentiate between the spin singlet and the triplet states. The repulsive contributions of the color magnetic interactions to the spin singlet state is larger than that for the triplet state. Thus the intermediate range attraction for the triplet state is larger than that for the singlet state. The OPEP also provides state independent repulsion. Thus, the intermediate range attraction in the singlet state is absent in the presence of the OPEP. The III provides a strong attractive contribution in the short range. The strength of the attraction is comparable to the strength of the repulsion provided by the OGEP in the short range. The direct part of the Hamiltonian is attractive in the short and intermediate ranges while the exchange part is repulsive in the short range. The exchange part of the Hamiltonian exhibits a small amount of attraction in the intermediate range.

4.2 Scope for future works

In this thesis, we have explained qualitatively the NN interaction potential in the framework of NRQM using RGM. The model successfully reproduces the qualitative features of the interaction potential. However, potentials are not the measurable quantities. The measurable quantity in any scattering reaction is the scattering cross-section. We have not attempted to calculate the scattering cross-section for the singlet and triplet NN scattering. Also of importance will be to calculate the mass spectrum of the $SU(2)$ baryons and their decay widths. The parameters of our model can then be used to re-calculate the NN potential and the scattering cross-section and also probe the importance of the Δ and the hidden color channel in the NN scattering. These calculations will provide valuable insights into the physics behind the NN scattering and hence the strong interactions.

Appendix A

Appendix: Matrix elements

In this section, we detail the procedure used to calculate the Hamiltonian matrix elements and list the various matrix elements.

A.1 Calculating the Matrix elements in RGM.

The RGM equation is given by

$$\langle \psi | (H - E) \mathcal{A} | \psi \rangle = 0$$

where, H and \mathcal{A} are the Hamiltonian (eq.2.1) and the anti-symmetrization (eq.2.19) operator respectively. The orbital part of the matrix elements can then be calculated as,

$$O_{ij} = \int \prod_{i=1}^6 d^3 r_i \phi^\dagger(\mathbf{r}_i) \mathcal{O}_{ij} \phi(\mathbf{r}_i) \quad (\text{A.1})$$

where \mathcal{O}_{ij} is any operator belonging to the orbital part of the Hamiltonian, and $\phi(\mathbf{r}_i)$ is the orbital part of the wave function.

As an example we calculate the matrix element corresponding to the direct and the exchange part of the Coulomb part of the OGEP with $i = 1$ and $j = 2$ *i.e.*, the matrix element of $\frac{\alpha_s}{4} \frac{1}{r_{12}}$ of the OGEP. We designate the matrix elements as V_{12Coul}^D and V_{12Coul}^E where D and E imply direct and exchange respectively.

$$\begin{aligned}
V_{12Coul}^D &= \frac{\alpha_s}{4} \int \prod_{i=1}^3 \frac{1}{(\pi b^2)^{(-3/4)}} \exp\left(-\frac{1}{2b^2}(\mathbf{r}_i - \frac{\mathbf{s}_I}{2})^2\right) \frac{1}{r_{12}} \frac{1}{(\pi b^2)^{(-3/4)}} \exp\left(-\frac{1}{2b^2}(\mathbf{r}_i + \frac{\mathbf{s}_I}{2})^2\right) \\
&\otimes \prod_{i=4}^6 \frac{1}{(\pi b^2)^{(-3/4)}} \exp\left(-\frac{1}{2b^2}(\mathbf{r}_i - \frac{\mathbf{s}_J}{2})^2\right) \frac{1}{(\pi b^2)^{(-3/4)}} \exp\left(-\frac{1}{2b^2}(\mathbf{r}_i + \frac{\mathbf{s}_J}{2})^2\right) \prod_{k=1}^6 d^3 \mathbf{r}_k
\end{aligned}$$

The integrals on $\mathbf{r}_i, i = 3, 4, 5, 6$ reduces to the normalization integral and are together denoted as d^4 where, $d = \exp(\frac{-1}{16b^2}(\mathbf{s}_I - \mathbf{s}_J)^2)$. Thus,

$$\begin{aligned}
V_{12Coul}^D &= \frac{\alpha_s}{4} d^4 \frac{1}{(\pi b^2)^{-3}} \int d^3 \mathbf{r}_1 d^3 \mathbf{r}_2 \frac{1}{r_{12}} \exp\left(-\frac{1}{2b^2}(\mathbf{r}_1 - \frac{\mathbf{s}_I}{2})^2\right) \exp\left(-\frac{1}{2b^2}(\mathbf{r}_2 - \frac{\mathbf{s}_I}{2})^2\right) \\
&\otimes \exp\left(-\frac{1}{2b^2}(\mathbf{r}_1 - \frac{\mathbf{s}_J}{2})^2\right) \exp\left(-\frac{1}{2b^2}(\mathbf{r}_2 - \frac{\mathbf{s}_J}{2})^2\right)
\end{aligned}$$

To solve the above integral, we make the transformation $\mathbf{r}_1 - \mathbf{r}_2 = \mathbf{r}$ and $\mathbf{R} = \frac{\mathbf{r}_1 + \mathbf{r}_2}{2}$. The integral is then given by,

$$\begin{aligned}
V_{12Coul}^D &= \frac{\alpha_s}{4} \frac{d^6}{b^3 \sqrt{8\pi^3}} \int \frac{1}{r} \exp\left(-\frac{r^2}{2b^2}\right) d^3 \mathbf{r} \\
&= \frac{\alpha_s}{4} \frac{d^6}{b} \sqrt{\frac{2}{\pi}}
\end{aligned}$$

The corresponding exchange matrix element is calculated as,

$$\begin{aligned}
V_{12Coul}^E &= \frac{\alpha_s}{4} \int \prod_{i=1}^3 \frac{1}{(\pi b^2)^{(-3/2)}} \exp\left(-\frac{1}{2b^2}(\mathbf{r}_i - \frac{\mathbf{s}_I}{2})^2\right) \frac{P_{36}^{OSTC}}{r_{12}} \exp\left(-\frac{1}{2b^2}(\mathbf{r}_i + \frac{\mathbf{s}_I}{2})^2\right) \\
&\otimes \prod_{i=4}^6 \frac{1}{(\pi b^2)^{(-3/2)}} \exp\left(-\frac{1}{2b^2}(\mathbf{r}_i - \frac{\mathbf{s}_J}{2})^2\right) \exp\left(-\frac{1}{2b^2}(\mathbf{r}_i + \frac{\mathbf{s}_J}{2})^2\right) \prod_{k=1}^6 d^3 \mathbf{r}_k
\end{aligned}$$

The operator P_{36}^{OSTC} exchanges \mathbf{r}_3 with \mathbf{r}_6 . The integrals on $\mathbf{r}_i, i = 3, 4, 5, 6$ reduce to the normalization integrals and are denoted by $d^2 e^2$ where, $d = \exp(\frac{-1}{16b^2}(\mathbf{s}_I - \mathbf{s}_J)^2)$ and $e = \exp(\frac{-1}{16b^2}(\mathbf{s}_I + \mathbf{s}_J)^2)$. The matrix element reduces to,

$$\begin{aligned}
V_{12Coul}^E &= \frac{\alpha_s}{4} d^2 e^2 \frac{1}{(\pi b^2)^{-3}} \int d^3 \mathbf{r}_1 d^3 \mathbf{r}_2 \frac{1}{r_{12}} \exp\left(-\frac{1}{2b^2}(\mathbf{r}_1 - \frac{\mathbf{s}_I}{2})^2\right) \exp\left(-\frac{1}{2b^2}(\mathbf{r}_2 - \frac{\mathbf{s}_I}{2})^2\right) \\
&\otimes \exp\left(-\frac{1}{2b^2}(\mathbf{r}_1 - \frac{\mathbf{s}_J}{2})^2\right) \exp\left(-\frac{1}{2b^2}(\mathbf{r}_2 - \frac{\mathbf{s}_J}{2})^2\right)
\end{aligned}$$

Using the transformations $\mathbf{r}_1 - \mathbf{r}_2 = \mathbf{r}$ and $\mathbf{R} = \frac{\mathbf{r}_1 + \mathbf{r}_2}{2}$, the integral reduces to,

$$\begin{aligned} V_{12Coul}^E &= \frac{\alpha_s}{4} \frac{d^4 e^2}{b^3 \sqrt{8\pi^3}} \int \frac{1}{r} \exp(-\frac{r^2}{2b^2}) d^3 \mathbf{r} \\ &= \frac{\alpha_s}{4} \frac{d^4 e^2}{b} \sqrt{\frac{2}{\pi}} \end{aligned}$$

These are projected onto the orbital angular momentum $l = 0$ state using the equation,

$$O_{ij}|_l = \int d\hat{\mathbf{s}}_I d\hat{\mathbf{s}}_J Y_{lm}^*(\hat{\mathbf{s}}_I) O_{ij} Y_{lm}(\hat{\mathbf{s}}_J)$$

Thus, the $l = 0$ projection of V_{12Coul}^D would be,

$$\begin{aligned} V_{12Coul}^D|_{l=0} &= \int d\hat{\mathbf{s}}_I d\hat{\mathbf{s}}_J Y_{00}^*(\hat{\mathbf{s}}_I) \frac{\alpha_s}{4} \frac{d^6}{b} \sqrt{\frac{2}{\pi}} Y_{00}(\hat{\mathbf{s}}_J) \\ &= \frac{\alpha_s}{4} \frac{1}{b} \sqrt{\frac{2}{\pi}} \int d\hat{\mathbf{s}}_I d\hat{\mathbf{s}}_J Y_{00}^*(\hat{\mathbf{s}}_I) d^6 Y_{00}(\hat{\mathbf{s}}_J) \\ &= \frac{\alpha_s}{4} \frac{1}{b} \sqrt{\frac{2}{\pi}} \int d\hat{\mathbf{s}}_I d\hat{\mathbf{s}}_J \exp(\frac{-1}{16b^2}(\mathbf{s}_I^2 - \mathbf{s}_J^2)) \\ &= \frac{\alpha_s}{4} \frac{1}{b} \sqrt{\frac{2}{\pi}} e^{(-\frac{3}{8} \frac{s_I^2 + s_J^2}{b^2})} \sinh(\frac{3s_I s_J}{4b^2}) \frac{4b^2}{3s_I s_J} \\ &= \frac{\alpha_s}{4} \sqrt{\frac{2}{\pi}} e^{(-\frac{3}{8} \frac{s_I^2 + s_J^2}{b^2})} \sinh(\frac{3s_I s_J}{4b^2}) \frac{4}{3bs_I s_J} \end{aligned}$$

Similarly,

$$V_{12Coul}^E|_{l=0} = \frac{\alpha_s}{4} \sqrt{\frac{2}{\pi}} e^{(-\frac{3}{8} \frac{s_I^2 + s_J^2}{b^2})} \sinh(\frac{s_I s_J}{4b^2}) \frac{4}{bs_I s_J}$$

Following the above procedure, we see that the projections of $N_D(= d^6)$ and $N_E(= d^4 e^2)$ are,

$$\begin{aligned} N_D|_{l=0} &= 4\pi e^{-\frac{3}{8} \frac{s_I^2 + s_J^2}{b^2}} \sinh(\frac{3s_I s_J}{4b^2}) \frac{4b^2}{3s_I s_J} \\ N_E|_{l=0} &= 4\pi e^{-\frac{3}{8} \frac{s_I^2 + s_J^2}{b^2}} \sinh(\frac{s_I s_J}{4b^2}) \frac{4b^2}{s_I s_J} \end{aligned}$$

A.1.1 Spin and Isospin matrix elements

The spin-isospin state of the NN system is given by,

$$|NN\rangle = \frac{1}{2} \sum_{s,t} |(s, \frac{1}{2}); (t, \frac{1}{2}); S, M_S\rangle \otimes |(s, \frac{1}{2}); (t, \frac{1}{2}); T, M_T\rangle$$

The spin-isospin matrix elements are,

$$\begin{aligned} \langle NN | O^{ST} P_{36}^S P_{36}^T | NN \rangle &= \frac{1}{4} \sum_{s_1, t_1; s_2, t_2} \langle (s_1, \frac{1}{2}); (s_2, \frac{1}{2}); S, M_S | O^S P_{36}^S | (s_1, \frac{1}{2}); (s_2, \frac{1}{2}); S, M_S \rangle \\ &\quad \otimes \langle (t_1, \frac{1}{2}); (t_2, \frac{1}{2}); T, M_T | O^T P_{36}^T | (t_1, \frac{1}{2}); (t_2, \frac{1}{2}); T, M_T \rangle \end{aligned}$$

For $O^T = 1$, the isospin matrix element reduces to the product of the 9J symbols.

In the presence of O^T , The exchange operator P_{ij} can be written as,

$$P_{ij}^T = \frac{1}{2} + \frac{\boldsymbol{\tau}_i \cdot \boldsymbol{\tau}_j}{2}$$

Hence the isospin operator can be written as,

$$\boldsymbol{\tau}_i \cdot \boldsymbol{\tau}_j = 2(P_{ij}^T - 1)$$

Similarly the spin operator can be written as,

$$\boldsymbol{\sigma}_i \cdot \boldsymbol{\sigma}_j = 2(P_{ij}^S - 1)$$

The values of the spin-isospin matrix elements for different values of i and j are given in table A.2

A.1.2 Color matrix elements

The color wave function is given by,

$$|C\rangle = [222] = \begin{array}{|c|c|} \hline \square & \square \\ \hline \square & \square \\ \hline \square & \square \\ \hline \end{array}$$

The color permutation operator P_{ij}^C can be written as,

$$P_{ij}^C = \frac{1}{3} + \frac{\lambda_i \cdot \lambda_j}{2}$$

Thus the color operator is,

$$\lambda_i \cdot \lambda_j = 2P_{ij}^C - \frac{2}{3}$$

Hence the color matrix elements are given by,

$$\langle C | \lambda_i \cdot \lambda_j P_{36}^C | C \rangle = \langle C | (2P_{ij}^C - \frac{2}{3}) P_{36}^C | C \rangle$$

The values of the color matrix elements for different values of i and j are listed in table A.2

A.1.3 Lists of Matrix elements.

The matrix elements corresponding to the above mentioned operators are listed in this section. A list of these operators is given in table A.1.

The kinetic energy of the quarks is given by,

$$K = \frac{-1}{2m^2} \sum_{i=1}^6 (\nabla_i^2 - \frac{-1}{12m^2} \nabla_R^2)$$

where, ∇_R^2 is the Laplacian with respect to the center of mass. The matrix elements are split into direct (D) and exchange (E) parts and the kinetic energy is further split into: K_D , K_{E1} , K_{E3} , K_D^{CM} , and K_E^{CM} . The matrix elements before projection are,

$$\begin{aligned} K_D &= \frac{3}{2mb^2} (1 - \frac{1}{24} \frac{(\mathbf{s}_I - \mathbf{s}_J)^2}{b^2}) N_D \\ K_{E1} &= \frac{3}{2mb^2} (1 - \frac{1}{24} \frac{(\mathbf{s}_I - \mathbf{s}_J)^2}{b^2}) N_E \\ K_{E3} &= \frac{3}{2mb^2} (1 - \frac{1}{24} \frac{(\mathbf{s}_I + \mathbf{s}_J)^2}{b^2}) N_E \\ K_D^{CM} &= \frac{3}{2mb^2} N_D \\ K_E^{CM} &= \frac{3}{2mb^2} N_E \end{aligned}$$

where, $N_D = d^6$ and $N_E = d^4 e^2$. The matrix elements after projection are,

$$\begin{aligned} K_D &= 4\pi \frac{3}{2mb^2} \exp(-\frac{s_I^2 + s_J^2}{b^2}) (\sinh(\frac{3s_I s_J}{4b^2}) \frac{4b^2}{3s_I s_J} - \frac{1}{24} \frac{(s_I - s_J)^2}{b^2} \sinh(\frac{3s_I s_J}{4b^2}) \frac{4b^2}{3s_I s_J} \\ &\quad + \frac{s_I s_J}{12b^2} (\frac{x \cosh(x) - \sinh(x)}{x^2})) \\ K_{E1} &= 4\pi \frac{3}{2mb^2} \exp(-\frac{s_I^2 + s_J^2}{b^2}) (\sinh(\frac{3s_I s_J}{4b^2}) \frac{4b^2}{s_I s_J} - \frac{1}{24} \frac{(s_I - s_J)^2}{b^2} \sinh(\frac{s_I s_J}{4b^2}) \frac{4b^2}{s_I s_J} \\ &\quad + \frac{s_I s_J}{12b^2} (\frac{y \cosh(y) - \sinh(y)}{x^2})) \\ K_{E3} &= 4\pi \frac{3}{2mb^2} \exp(-\frac{s_I^2 + s_J^2}{b^2}) (\sinh(\frac{3s_I s_J}{4b^2}) \frac{4b^2}{s_I s_J} - \frac{1}{24} \frac{(s_I - s_J)^2}{b^2} \sinh(\frac{s_I s_J}{4b^2}) \frac{4b^2}{s_I s_J} \\ &\quad - \frac{s_I s_J}{12b^2} (\frac{y \cosh(y) - \sinh(y)}{x^2})) \\ K_D^{CM} &= \frac{3}{2mb^2} N_D|_{l=0} \\ K_E^{CM} &= \frac{3}{2mb^2} N_E|_{l=0} \end{aligned}$$

where, $x = \frac{3}{4} \frac{s_I s_J}{b^2}$ and $y = \frac{1}{4} \frac{s_I s_J}{b^2}$
The Coulomb part of OGEP,

$$V_{Coul} = \frac{\alpha_s}{4} \sum_{i < j} \frac{1}{r_{ij}}$$

Before projection

$$\begin{aligned} V_{12}^D &= \frac{\alpha_s}{4} \frac{1}{b} \sqrt{\frac{2}{\pi}} N_D \\ V_{12}^E &= \frac{\alpha_s}{4} \frac{1}{b} \sqrt{\frac{2}{\pi}} N_E \\ V_{13}^E &= \frac{\alpha_s}{4} \frac{2}{s_J} \text{Erf}\left(\frac{s_J}{\sqrt{8b}}\right) N_E \\ V_{16}^E &= \frac{\alpha_s}{4} \frac{2}{s_I} \text{Erf}\left(\frac{s_I}{\sqrt{8b}}\right) N_E \\ V_{14}^E &= \frac{\alpha_s}{4} \frac{2}{s_I + s_J} \text{Erf}\left(\frac{s_I + s_J}{\sqrt{8b}}\right) N_E \\ V_{36}^E &= \frac{\alpha_s}{4} \frac{2}{s_I - s_J} \text{Erf}\left(\frac{s_I - s_J}{\sqrt{8b}}\right) N_E \end{aligned}$$

where the error function $\text{Erf}(x)$ is defined as,

$$\text{Erf}(x) = \frac{2}{\sqrt{\pi}} \int_0^x e^{-y^2} dy$$

After projection

$$\begin{aligned} V_{12}^D &= \frac{\alpha_s}{4} \frac{1}{b} \sqrt{\frac{2}{\pi}} N_D|_{l=0} \\ V_{12}^E &= \frac{\alpha_s}{4} \frac{1}{b} \sqrt{\frac{2}{\pi}} N_E|_{l=0} \\ V_{13}^E &= \frac{\alpha_s}{4} \frac{2}{s_J} \text{Erf}\left(\frac{s_J}{\sqrt{8b}}\right) N_E|_{l=0} \\ V_{16}^E &= \frac{\alpha_s}{4} \frac{2}{s_I} \text{Erf}\left(\frac{s_I}{\sqrt{8b}}\right) N_E|_{l=0} \\ V_{14}^E &= \frac{\alpha_s}{4} \frac{2}{s_I + s_J} \text{Erf}\left(\frac{s_I + s_J}{\sqrt{8b}}\right) N_E|_{l=0} \\ V_{36}^E &= \frac{\alpha_s}{4} \frac{2}{s_I - s_J} \text{Erf}\left(\frac{s_I - s_J}{\sqrt{8b}}\right) N_E|_{l=0} \end{aligned}$$

The color electric part of OGEP is

$$V_{CE} = -\frac{\alpha_s}{4} \frac{\pi}{m^2} \sum_{i < j} \delta(\mathbf{r}_{ij})$$

Before projection

$$\begin{aligned} V_{12}^D &= \frac{\alpha_s}{4} \frac{\pi}{m^2} \frac{1}{b^3} \sqrt{\frac{2}{\pi^3}} N_D \\ V_{12}^E &= \frac{\alpha_s}{4} \frac{\pi}{m^2} \frac{1}{b^3} \sqrt{\frac{2}{\pi^3}} N_E \\ V_{13}^E &= \frac{\alpha_s}{4} \frac{\pi}{m^2} \frac{1}{b^3} \sqrt{\frac{2}{\pi^3}} e^{(-\frac{s_J^2}{8b^2})} N_E \\ V_{16}^E &= \frac{\alpha_s}{4} \frac{\pi}{m^2} \frac{1}{b^3} \sqrt{\frac{2}{\pi^3}} e^{(-\frac{s_I^2}{8b^2})} N_E \\ V_{14}^E &= \frac{\alpha_s}{4} \frac{\pi}{m^2} \frac{1}{b^3} \sqrt{\frac{2}{\pi^3}} e^{(-\frac{(s_I+s_J)^2}{2b^2})} N_E \\ V_{36}^E &= \frac{\alpha_s}{4} \frac{\pi}{m^2} \frac{1}{b^3} \sqrt{\frac{2}{\pi^3}} e^{(-\frac{(s_I-s_J)^2}{2b^2})} N_E \end{aligned}$$

After projection

$$\begin{aligned} V_{12}^D &= \frac{\alpha_s}{4} \frac{\pi}{m^2} \frac{1}{b^3} \sqrt{\frac{2}{\pi^3}} N_D|_{l=0} \\ V_{12}^E &= \frac{\alpha_s}{4} \frac{\pi}{m^2} \frac{1}{b^3} \sqrt{\frac{2}{\pi^3}} N_E|_{l=0} \\ V_{13}^E &= \frac{\alpha_s}{4} \frac{\pi}{m^2} \frac{1}{b^3} \sqrt{\frac{2}{\pi^3}} \exp(-\frac{s_J^2}{8b^2}) N_E|_{l=0} \\ V_{16}^E &= \frac{\alpha_s}{4} \frac{\pi}{m^2} \frac{1}{b^3} \sqrt{\frac{2}{\pi^3}} \exp(-\frac{s_I^2}{8b^2}) N_E|_{l=0} \\ V_{14}^E &= \frac{4}{\pi} \frac{\alpha_s}{4} \frac{\pi}{m^2} \frac{1}{b^3} \sqrt{\frac{2}{\pi^3}} \exp(-\frac{s_I^2 + s_J^2}{b^2}) \sinh(\frac{s_I s_J}{b^2}) \frac{b^2}{s_I s_J} \\ V_{36}^E &= \frac{4}{\pi} \frac{\alpha_s}{4} \frac{\pi}{m^2} \frac{1}{b^3} \sqrt{\frac{2}{\pi^3}} \exp(-\frac{s_I^2 + s_J^2}{b^2}) \sinh(\frac{3s_I s_J}{2b^2}) \frac{2b^2}{3s_I s_J} \end{aligned}$$

The corresponding color magnetic elements are to be multiplied by $\frac{-2}{3}$. The orbital matrix elements of the III potential are similar to the ones listed above. The color independent part of the III have the multiplier $-\frac{W}{2} \frac{16}{15}$, the color electric matrix elements have $-\frac{W}{2} \frac{2}{5}$ and the color magnetic components $-\frac{W}{2} \frac{1}{10}$ instead of $\frac{\alpha_s}{4} \frac{\pi}{m^2}$ of the OGEP. The OPEP potential is,

$$V_{OPEP} = \frac{f_Q^2}{3} \sum_{i < j} \frac{e^{-m_\pi r_{ij}}}{r_{ij}}$$

Before projection

$$\begin{aligned} V_{12}^D &= \frac{f_Q^2}{3} \frac{N_D}{b} \sqrt{\frac{2}{\pi}} \left(1 - m_\pi b \sqrt{\frac{\pi}{2}} e^{m_\pi^2 \frac{b^2}{2}} \text{Erfc} \left[\frac{m_\pi b}{\sqrt{2}} \right] \right) \\ V_{36}^D &= \left(e^{2(\frac{s_I+s_J}{4})m_\pi} \text{Erfc} \left[\frac{2(\frac{s_I+s_J}{4}) + m_\pi b^2}{\sqrt{2}b} \right] - e^{-2(\frac{s_I+s_J}{4})m_\pi} \text{Erfc} \left[\frac{-2(\frac{s_I+s_J}{4}) + m_\pi b^2}{\sqrt{2}b} \right] \right) \\ &\quad \otimes \frac{f_Q^2}{3} \frac{N_D}{(\frac{s_I+s_J}{4})} \sqrt{2} e^{m_\pi^2 \frac{b^2}{2}} \\ V_{12}^E &= \frac{f_Q^2}{3} \frac{N_E}{b} \sqrt{\frac{2}{\pi}} \left(1 - m_\pi b \sqrt{\frac{\pi}{2}} e^{m_\pi^2 \frac{b^2}{2}} \text{Erfc} \left[\frac{m_\pi b}{\sqrt{2}} \right] \right) \\ V_{36}^E &= \left(e^{2(\frac{s_I-s_J}{4})m_\pi} \text{Erfc} \left[\frac{2(\frac{s_I-s_J}{4}) + m_\pi b^2}{\sqrt{2}b} \right] - e^{-2(\frac{s_I-s_J}{4})m_\pi} \text{Erfc} \left[\frac{-2(\frac{s_I-s_J}{4}) + m_\pi b^2}{\sqrt{2}b} \right] \right) \\ &\quad \otimes \frac{f_Q^2}{3} \frac{N_E}{(\frac{s_I-s_J}{4})} \sqrt{2} e^{m_\pi^2 \frac{b^2}{2}} \\ V_{13}^E &= \frac{f_Q^2}{3} \frac{N_E}{s_J} 4\sqrt{2} e^{m_\pi^2 \frac{b^2}{2}} \left(e^{\frac{s_J m_\pi}{2}} \text{Erfc} \left[\frac{\frac{s_J}{2} + m_\pi b^2}{\sqrt{2}b} \right] - e^{-\frac{s_J}{2} m_\pi} \text{Erfc} \left[\frac{-\frac{s_J}{2} + m_\pi b^2}{\sqrt{2}b} \right] \right) \\ V_{16}^E &= \frac{f_Q^2}{3} \frac{N_E}{s_I} 4\sqrt{2} e^{m_\pi^2 \frac{b^2}{2}} \left(e^{\frac{s_I m_\pi}{2}} \text{Erfc} \left[\frac{\frac{s_I}{2} + m_\pi b^2}{\sqrt{2}b} \right] - e^{-\frac{s_I}{2} m_\pi} \text{Erfc} \left[\frac{-\frac{s_I}{2} + m_\pi b^2}{\sqrt{2}b} \right] \right) \\ V_{14}^E &= \left(e^{2(\frac{s_I+s_J}{4})m_\pi} \text{Erfc} \left[\frac{2(\frac{s_I+s_J}{4}) + m_\pi b^2}{\sqrt{2}b} \right] - e^{-2(\frac{s_I+s_J}{4})m_\pi} \text{Erfc} \left[\frac{-2(\frac{s_I+s_J}{4}) + m_\pi b^2}{\sqrt{2}b} \right] \right) \\ &\quad \otimes \frac{f_Q^2}{3} \frac{N_E}{(\frac{s_I+s_J}{4})} \sqrt{2} e^{m_\pi^2 \frac{b^2}{2}} \end{aligned}$$

After projection

$$\begin{aligned}
V_{12}^D &= \frac{f_Q^2}{3} \frac{N_D}{b} \sqrt{\frac{2}{\pi}} \left(1 - m_\pi b \sqrt{\frac{\pi}{2}} e^{m_\pi^2 \frac{b^2}{2}} \operatorname{Erfc} \left[\frac{m_\pi b}{\sqrt{2}} \right] \right) \Big|_{l=0} \\
V_{36}^D &= \left(e^{2(\frac{s_I+s_J}{4})m_\pi} \operatorname{Erfc} \left[\frac{2(\frac{s_I+s_J}{4}) + m_\pi b^2}{\sqrt{2}b} \right] - e^{-2(\frac{s_I+s_J}{4})m_\pi} \operatorname{Erfc} \left[\frac{-2(\frac{s_I+s_J}{4}) + m_\pi b^2}{\sqrt{2}b} \right] \right) \\
&\quad \otimes \frac{f_Q^2}{3} \frac{N_D}{(\frac{s_I+s_J}{4})} \sqrt{2} e^{m_\pi^2 \frac{b^2}{2}} \Big|_{l=0} \\
V_{12}^E &= \frac{f_Q^2}{3} \frac{N_E}{b} \sqrt{\frac{2}{\pi}} \left(1 - m_\pi b \sqrt{\frac{\pi}{2}} e^{m_\pi^2 \frac{b^2}{2}} \operatorname{Erfc} \left[\frac{m_\pi b}{\sqrt{2}} \right] \right) \Big|_{l=0} \\
V_{36}^E &= \left(e^{2(\frac{s_I-s_J}{4})m_\pi} \operatorname{Erfc} \left[\frac{2(\frac{s_I-s_J}{4}) + m_\pi b^2}{\sqrt{2}b} \right] - e^{-2(\frac{s_I-s_J}{4})m_\pi} \operatorname{Erfc} \left[\frac{-2(\frac{s_I-s_J}{4}) + m_\pi b^2}{\sqrt{2}b} \right] \right) \\
&\quad \otimes \frac{f_Q^2}{3} \frac{N_E}{(\frac{s_I-s_J}{4})} \sqrt{2} e^{m_\pi^2 \frac{b^2}{2}} \Big|_{l=0} \\
V_{13}^E &= \frac{f_Q^2}{3} \frac{N_E}{s_J} 4\sqrt{2} e^{m_\pi^2 \frac{b^2}{2}} \left(e^{\frac{s_J m_\pi}{2}} \operatorname{Erfc} \left[\frac{\frac{s_J}{2} + m_\pi b^2}{\sqrt{2}b} \right] - e^{-\frac{s_J}{2} m_\pi} \operatorname{Erfc} \left[\frac{-\frac{s_J}{2} + m_\pi b^2}{\sqrt{2}b} \right] \right) \Big|_{l=0} \\
V_{16}^E &= \frac{f_Q^2}{3} \frac{N_E}{s_I} 4\sqrt{2} e^{m_\pi^2 \frac{b^2}{2}} \left(e^{\frac{s_I m_\pi}{2}} \operatorname{Erfc} \left[\frac{\frac{s_I}{2} + m_\pi b^2}{\sqrt{2}b} \right] - e^{-\frac{s_I}{2} m_\pi} \operatorname{Erfc} \left[\frac{-\frac{s_I}{2} + m_\pi b^2}{\sqrt{2}b} \right] \right) \Big|_{l=0} \\
V_{14}^E &= \left(e^{2(\frac{s_I+s_J}{4})m_\pi} \operatorname{Erfc} \left[\frac{2(\frac{s_I+s_J}{4}) + m_\pi b^2}{\sqrt{2}b} \right] - e^{-2(\frac{s_I+s_J}{4})m_\pi} \operatorname{Erfc} \left[\frac{-2(\frac{s_I+s_J}{4}) + m_\pi b^2}{\sqrt{2}b} \right] \right) \\
&\quad \otimes \frac{f_Q^2}{3} \frac{N_E}{(\frac{s_I+s_J}{4})} \sqrt{2} e^{m_\pi^2 \frac{b^2}{2}} \Big|_{l=0}
\end{aligned}$$

The confinement potential is,

$$V_{CONF} = a_c \sum_{i < j} r_{ij}^2 \boldsymbol{\lambda}_i \cdot \boldsymbol{\lambda}_j$$

Before projection

$$\begin{aligned}
V_{12}^D &= a_c 3b^2 N_D \\
V_{12}^E &= a_c 3b^2 N_E \\
V_{13}^E &= a_c 3b^2 \left(1 + \frac{s_J^2}{12b^2} \right) N_E \\
V_{16}^E &= a_c 3b^2 \left(1 + \frac{s_I^2}{12b^2} \right) N_E \\
V_{14}^E &= a_c 3b^2 \left(1 + \frac{(\mathbf{s}_I + \mathbf{s}_J)^2}{12b^2} \right) N_E \\
V_{36}^E &= a_c 3b^2 \left(1 + \frac{(\mathbf{s}_I - \mathbf{s}_J)^2}{12b^2} \right) N_E
\end{aligned}$$

After projection

$$\begin{aligned}
V_{12}^D &= a_c 3b^2 N_D|_{l=0} \\
V_{12}^E &= a_c 3b^2 N_E|_{l=0} \\
V_{13}^E &= a_c 3b^2 \left(1 + \frac{s_J^2}{12b^2}\right) N_E|_{l=0} \\
V_{16}^E &= a_c 3b^2 \left(1 + \frac{s_I^2}{12b^2}\right) N_E|_{l=0} \\
V_{14}^E &= a_c 3b^2 4\pi \left[\left(1 + \frac{(s_I + s_J)^2}{12b^2}\right) N_E|_{l=0} \right. \\
&\quad \left. + \left(\frac{s_I s_J}{6b^2} e^{-\frac{3(s_I^2 + s_J^2)}{8b^2}} \frac{8b^2}{s_I s_J} \left(\cosh\left(\frac{s_I s_J}{4b^2}\right) - \frac{4b^2}{s_I s_J} \sinh\left(\frac{s_I s_J}{4b^2}\right)\right)\right) \right] \\
V_{36}^E &= a_c 3b^2 4\pi \left[\left(1 + \frac{(s_I + s_J)^2}{12b^2}\right) N_E|_{l=0} \right. \\
&\quad \left. - \left(\frac{s_I s_J}{6b^2} e^{-\frac{3(s_I^2 + s_J^2)}{8b^2}} \frac{8b^2}{s_I s_J} \left(\cosh\left(\frac{s_I s_J}{4b^2}\right) - \frac{4b^2}{s_I s_J} \sinh\left(\frac{s_I s_J}{4b^2}\right)\right)\right) \right]
\end{aligned}$$

The direct matrix elements are multiplied by $\frac{1}{10}$ and the exchange matrix elements by $\frac{-9}{10}$. The sum of all the matrix elements must be divided by the normalization kernel $\frac{1}{10}(N_D - 9N_E)|_{l=0}$. This gives the NN potential as a function of the NN separation s_I .

Operator	\mathcal{O}_{ij}
Kinetic energy	$\frac{\nabla_i^2}{2m_q}$
Coulomb part of OGEP	$\frac{\alpha_s}{4} \frac{1}{r_{ij}}$
Color electric part of OGEP	$\frac{\alpha_s}{4} \frac{\pi}{m_q^2} \delta(\mathbf{r}_{ij})$
Color magnetic part of OGEP	$-\frac{2}{3} \frac{\alpha_s}{4} \frac{\pi}{m_q^2} \delta(\mathbf{r}_{ij})$
Color independent part of III	$-\frac{W}{2} \frac{16}{15} \delta(\mathbf{r}_{ij})$
Color electric part of III	$-\frac{2}{5} \frac{W}{2} \delta(\mathbf{r}_{ij})$
Color magnetic part of III	$-\frac{1}{10} \frac{2}{3} \frac{W}{2} \delta(\mathbf{r}_{ij})$
Confinement	$a_c \mathbf{r}_{ij}^2$
OPEP	$\frac{f_Q^2}{3} \frac{\exp(-m_\pi r_{ij})}{r_{ij}}$

Table A.1: Different operators of the Hamiltonian

$\lambda_i.\lambda_j \sigma_i.\sigma_j \tau_i.\tau_j P_{36}^{STC}$	$S = 0$ $T = 1$	$S = 1$ $T = 0$
1	243	243
$\lambda_1.\lambda_2$	-648	-648
$\lambda_3.\lambda_6$	0	0
$\lambda_1.\lambda_2 \sigma_1.\sigma_2$	648	648
$\lambda_3.\lambda_6 \sigma_3.\sigma_6$	0	0
P_{36}^{STC}	-3	-3
$\lambda_1.\lambda_2 P_{36}^{STC}$	8	8
$\lambda_1.\lambda_3 P_{36}^{STC}$	8	8
$\lambda_1.\lambda_6 P_{36}^{STC}$	8	8
$\lambda_1.\lambda_4 P_{36}^{STC}$	-4	-4
$\lambda_3.\lambda_6 P_{36}^{STC}$	-16	-16
$\lambda_1.\lambda_2 \sigma_1.\sigma_2 P_{36}^{STC}$	-136	-136
$\lambda_1.\lambda_3 \sigma_1.\sigma_3 P_{36}^{STC}$	56	56
$\lambda_1.\lambda_6 \sigma_1.\sigma_6 P_{36}^{STC}$	56	56
$\lambda_1.\lambda_4 \sigma_1.\sigma_4 P_{36}^{STC}$	0	8
$\lambda_3.\lambda_6 \sigma_3.\sigma_6 P_{36}^{STC}$	496	304
$\sigma_1.\sigma_2 \tau_1.\tau_2$	1215	1215
$\sigma_3.\sigma_6 \tau_3.\tau_6$	-225	-225
$\sigma_1.\sigma_2 \tau_1.\tau_2 P_{36}^{STC}$	-333	-333
$\sigma_1.\sigma_3 \tau_1.\tau_3 P_{36}^{STC}$	99	99
$\sigma_1.\sigma_6 \tau_1.\tau_6 P_{36}^{STC}$	99	99
$\sigma_1.\sigma_4 \tau_1.\tau_4 P_{36}^{STC}$	27	27
$\sigma_3.\sigma_6 \tau_3.\tau_6 P_{36}^{STC}$	531	531

Table A.2: Color, spin and isospin matrix elements

Appendix B

Appendix: Plots

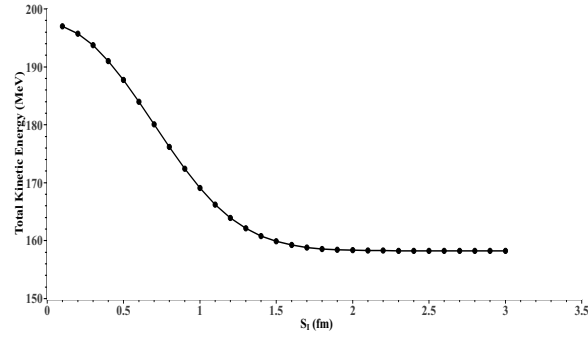


Figure B.1: Total kinetic energy.

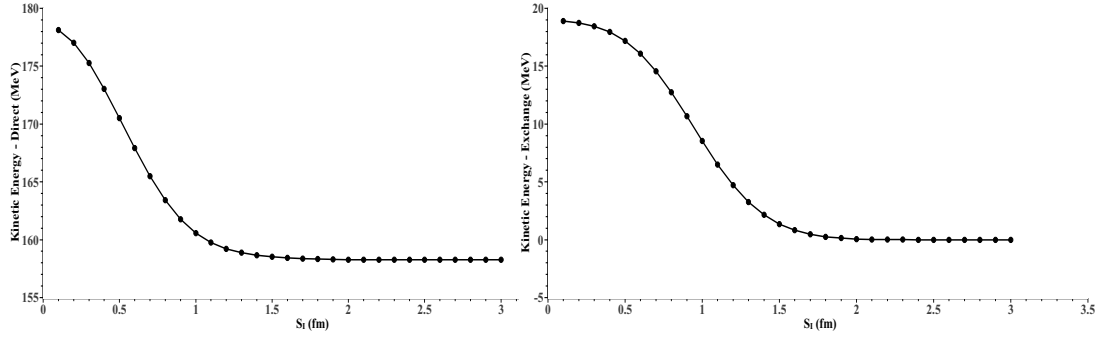


Figure B.2: Direct part of the kinetic energy. Figure B.3: Exchange part of the kinetic energy.

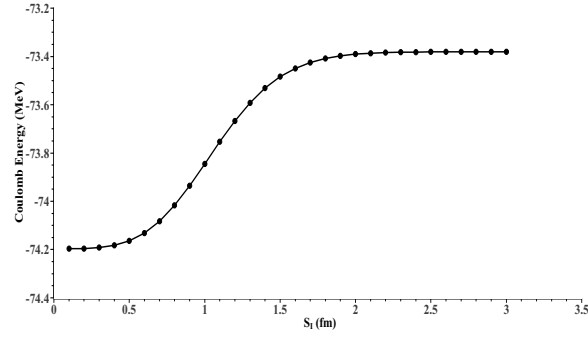


Figure B.4: Total Coulomb energy from OGEP.

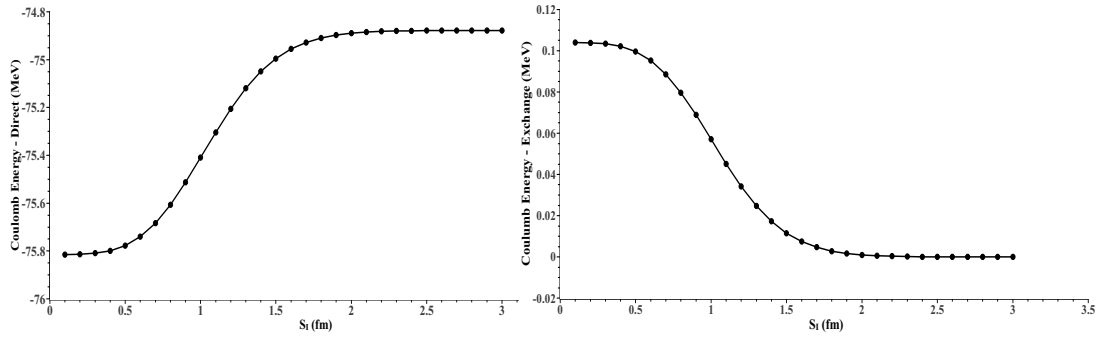


Figure B.5: Direct part of the Coulomb energy from OGEP. Figure B.6: Exchange part of the Coulomb energy from OGEP.

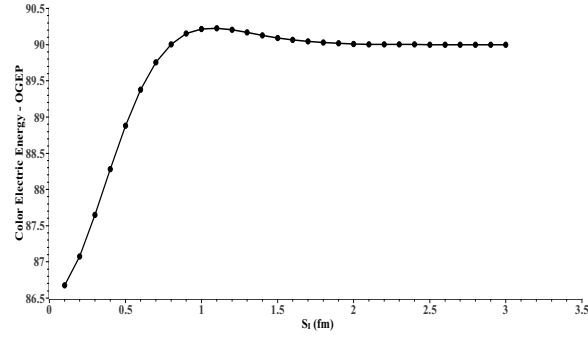


Figure B.7: Total color electric energy from OGEP.

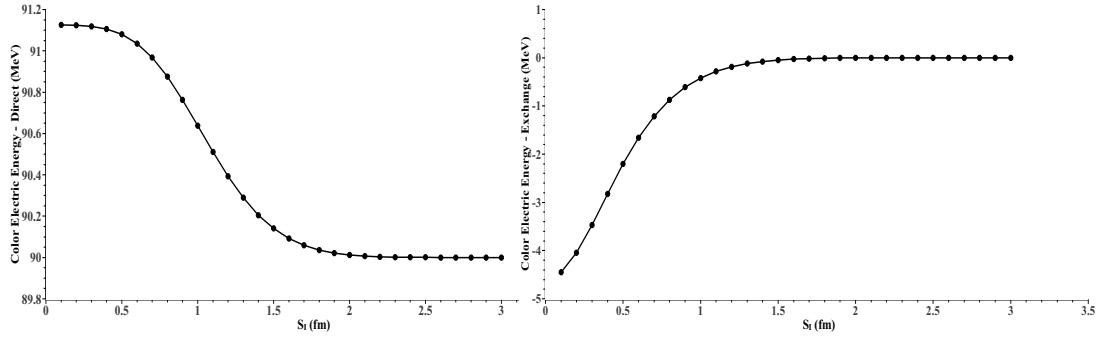


Figure B.8: Direct part of the color electric energy from OGEP. Figure B.9: Exchange part of the color electric energy from OGEP.

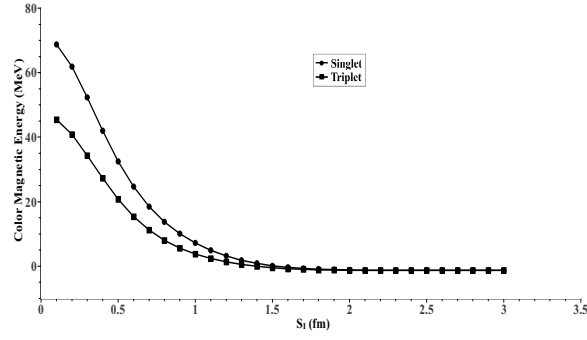


Figure B.10: Total color magnetic energy from OGEP.

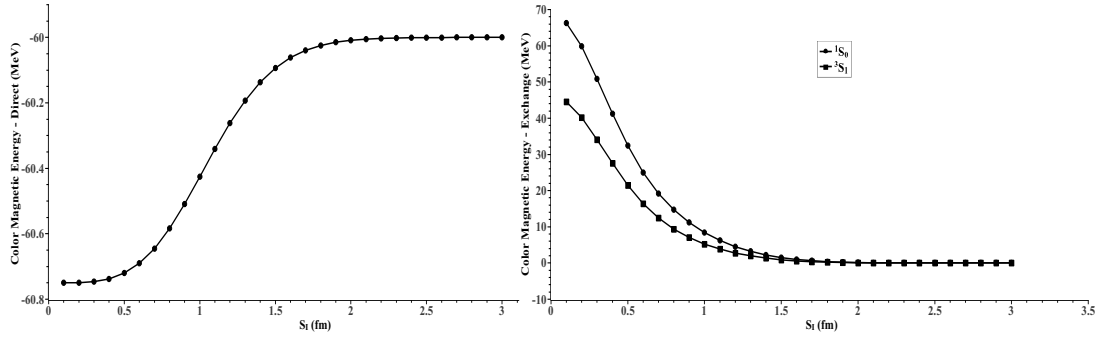


Figure B.11: Direct part of the color magnetic energy from OGEP.

Figure B.12: Exchange part of the color magnetic energy from OGEP.

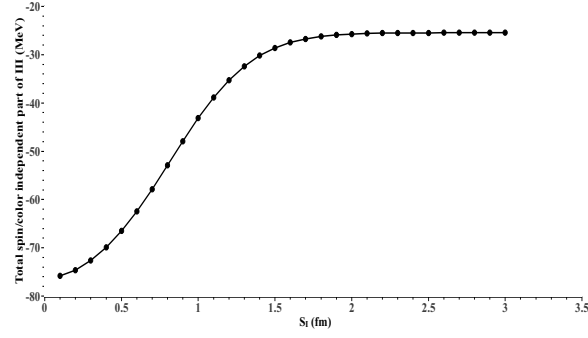


Figure B.13: Total energy from color independent part of III.

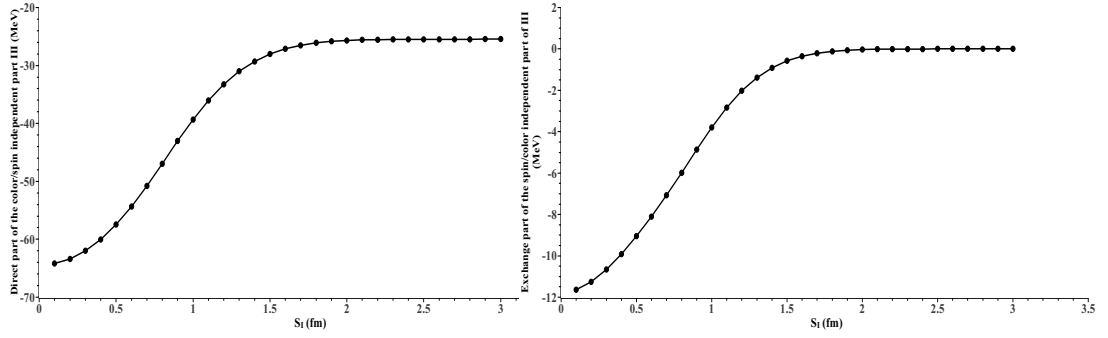


Figure B.14: Direct part of the color independent part of III. Figure B.15: Exchange part of the color independent part of III.

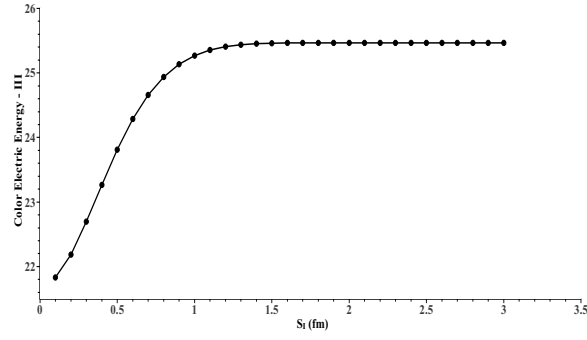


Figure B.16: Total color electric energy from III.

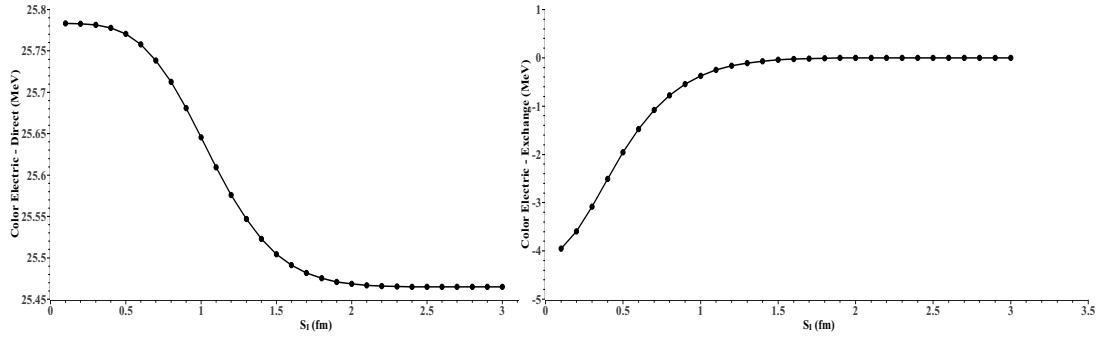


Figure B.17: Direct part of the color electric energy from III.

Figure B.18: Exchange part of the color electric energy from III.

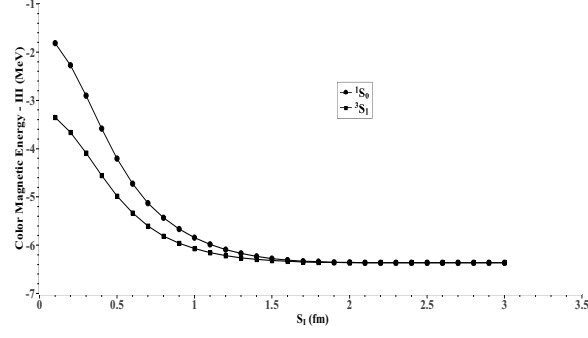


Figure B.19: Total color magnetic energy from III.

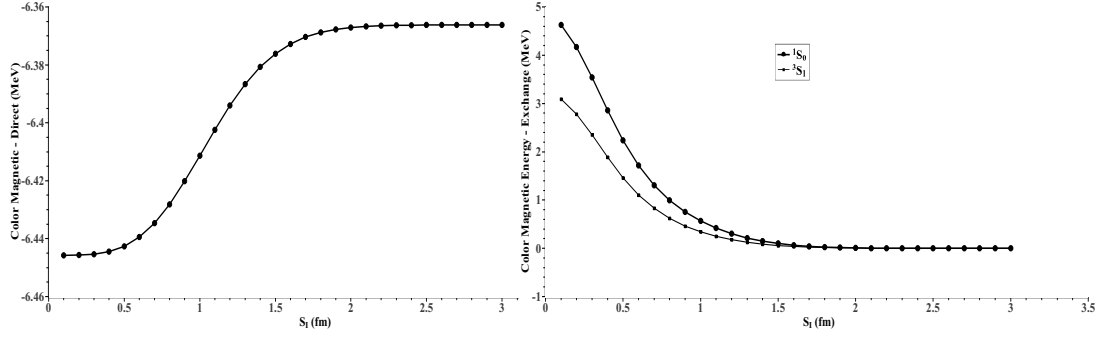


Figure B.20: Direct part of the color magnetic energy from III.

Figure B.21: Exchange part of the color magnetic energy from III.

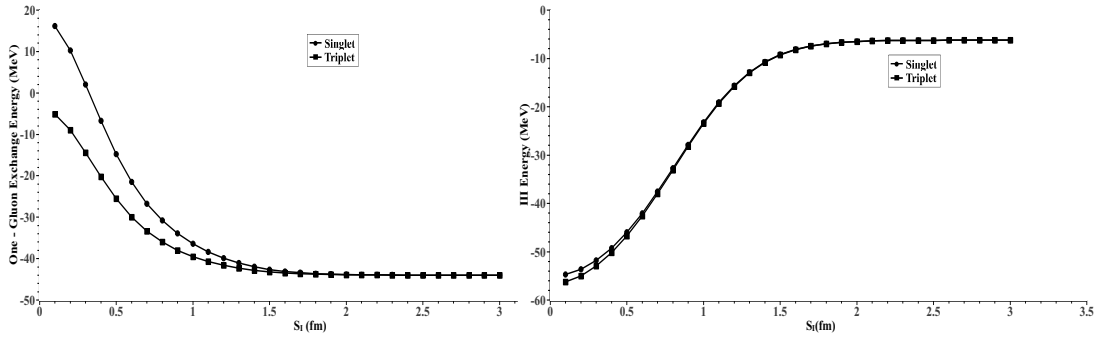


Figure B.22: Total contribution from OGE.

Figure B.23: Total contribution from III.

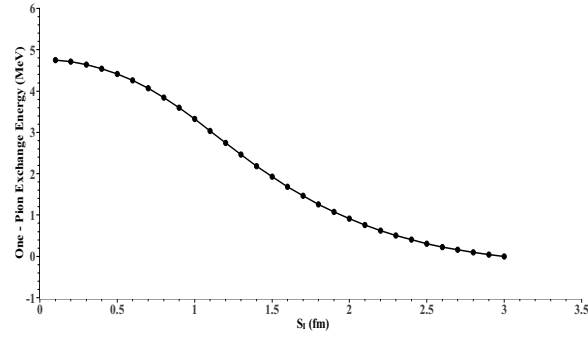


Figure B.24: Total OPEP energy.

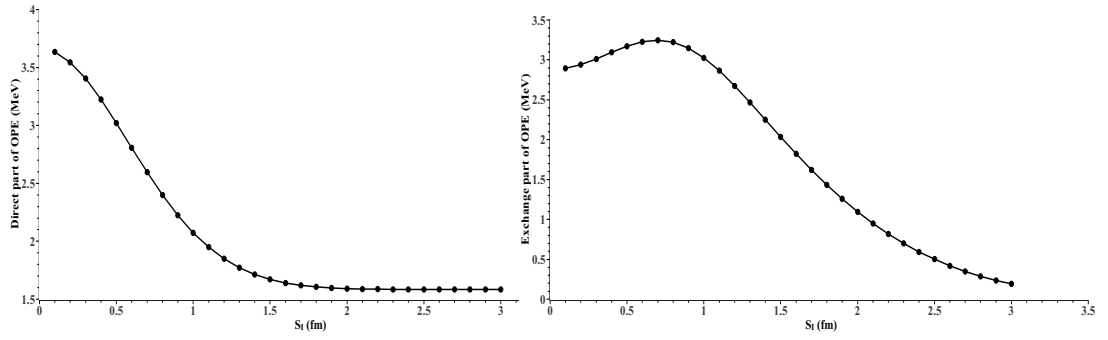


Figure B.25: Direct part of the OPEP energy.

Figure B.26: Exchange part of the OPEP energy.

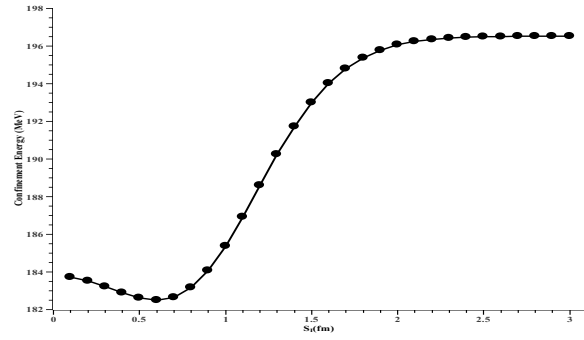


Figure B.27: Total Confinement energy.

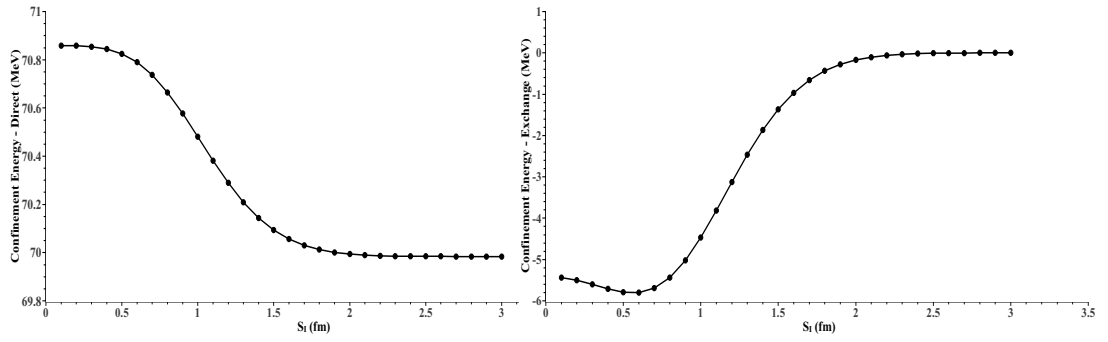


Figure B.28: Direct part of the confinement energy.

Figure B.29: Exchange part of the confinement energy.

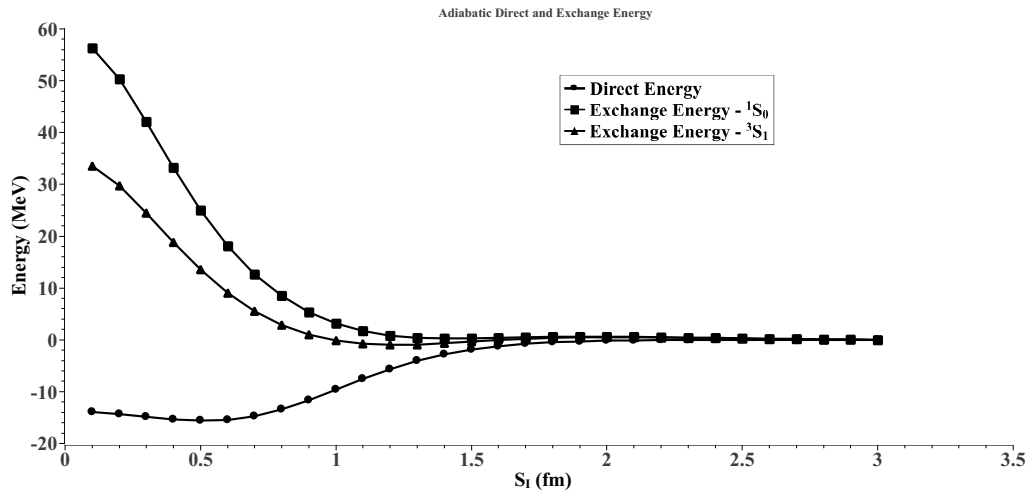


Figure B.30: Direct and exchange parts of the Hamiltonian in the adiabatic limit.

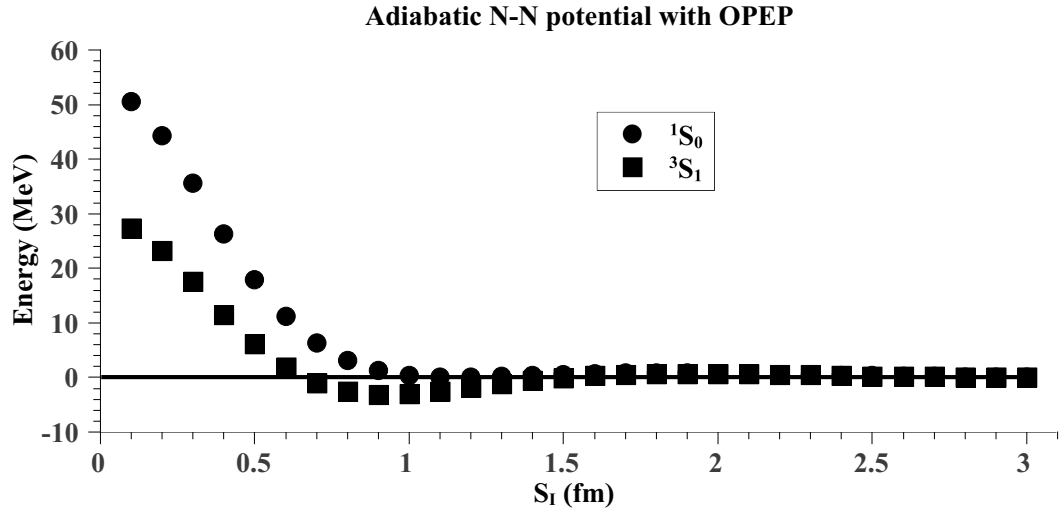


Figure B.31: NN potential with OPEP.

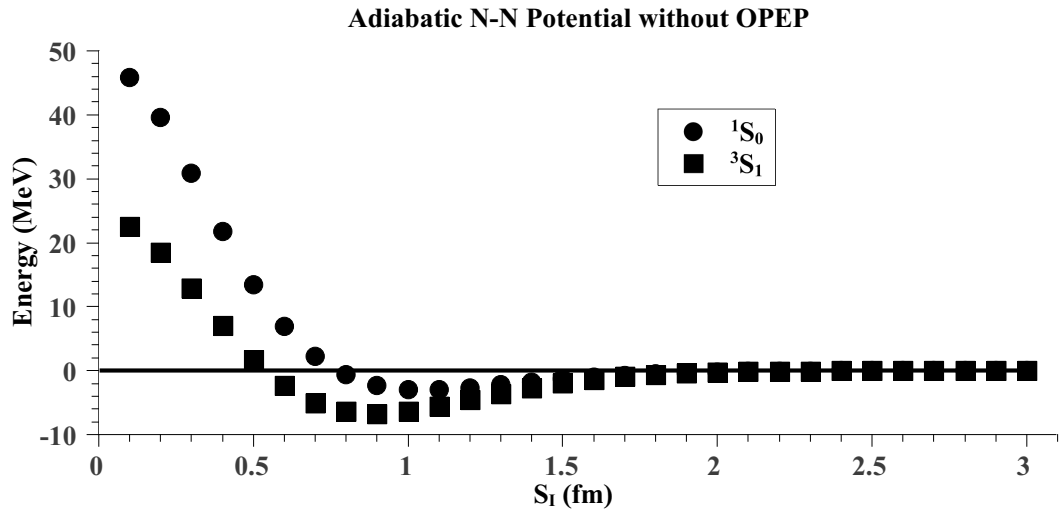


Figure B.32: NN potential without OPEP.

Bibliography

- [1] K. A. Olive et al. *Chin. Phys.*, C38:090001, 2014.
- [2] Mohammad Naghdi. *Phys. Part. Nucl.*, 45:924–971, 2014.
- [3] Hideki Yukawa. *Proc. Phys. Math. Soc. Jap.*, 17:48–57, 1935. [Prog. Theor. Phys. Suppl.1,1(1935)].
- [4] Solomon Gartenhaus. *Phys. Rev.*, 100:900–905, 1955.
- [5] K. A. Brueckner and K. M. Watson. *Phys. Rev.*, 92:1023–1035, 1953.
- [6] P. S. Signell and R. E. Marshak. *Phys. Rev.*, 106:832–834, 1957.
- [7] Mitsuo Taketani, Shigeru Machida, and Shoroku O-numa. *Progress of Theoretical Physics*, 7(1):45, 1952.
- [8] S. Okubo and R. E. Marshak. *Annals. Phys.*, 4:166, 1958.
- [9] T. Hamada and I. D. Johnston. *Nucl. Phys.*, 34:382–403, 1962.
- [10] K. E. Lassila, M. H. Hull, H. M. Ruppel, F. A. McDonald, and G. Breit. *Phys. Rev.*, 126:881–882, 1962.
- [11] Roderick V. Reid, Jr. *Annals Phys.*, 50:411–448, 1968.
- [12] B. D. Day. *Phys. Rev.*, C24:1203–1271, 1981.
- [13] W. N. Cottingham, M. Lacombe, B. Loiseau, J. M. Richard, and R. Vinh Mau. *Phys. Rev.*, D8:800–819, 1973.
- [14] I. E. Lagaris and V. R. Pandharipande. *Nucl. Phys.*, A359:331–348, 1981.
- [15] Robert B. Wiringa, R. A. Smith, and T. L. Ainsworth. *Phys. Rev.*, C29:1207–1221, 1984.
- [16] A. Scotti and D. Y. Wong. *Phys. Rev.*, 138:B145–B162, 1965.

- [17] G. Breit. *Phys. Rev.*, 120:287–292, 1960.
- [18] J. J. Sakurai. *Phys. Rev.*, 119:1784, 1960.
- [19] R. Machleidt, K. Holinde, and C. Elster. *Phys. Rept.*, 149:1–89, 1987.
- [20] R. Machleidt. *Adv. Nucl. Phys.*, 19:189–376, 1989.
- [21] R. Machleidt. *Phys. Rev.*, C63:024001, 2001.
- [22] J. R. Bergervoet, P. C. van Campen, R. A. M. Klomp, J. L. de Kok, T. A. Rijken, V. G. J. Stoks, and J. J. de Swart. *Phys. Rev.*, C41:1435–1452, 1990.
- [23] R. Timmermans, T. A. Rijken, and J. J. de Swart. *Phys. Rev.*, C50:48–73, 1994.
- [24] M. M. Nagels, T. A. Rijken, and J. J. De Swart. *Annals Phys.*, 79:338–385, 1973.
- [25] J. J. de Swart, R. A. M. M. Klomp, M. C. M. Rentmeester, and T. A. Rijken. *Few Body Syst. Suppl.*, 8:438–447, 1995.
- [26] Martin Breidenbach, Jerome I. Friedman, Henry W. Kendall, Elliott D. Bloom, D. H. Coward, H. C. DeStaebler, J. Drees, Luke W. Mo, and Richard E. Taylor. *Phys. Rev. Lett.*, 23:935–939, 1969.
- [27] G. von Gehlen. *Phys. Rev.*, 118:1455, 1960.
- [28] J. D. Bjorken. *Phys. Rev.*, 179:1547–1553, 1969.
- [29] D. J. Gross and Frank Wilczek. *Phys. Rev.*, D8:3633–3652, 1973.
- [30] D. J. Gross and Frank Wilczek. *Phys. Rev.*, D9:980–993, 1974.
- [31] H. David Politzer. *Phys. Rev. Lett.*, 30:1346–1349, 1973.
- [32] Murray Gell-Mann. *Phys. Lett.*, 8:214–215, 1964.
- [33] Murray Gell-Mann. *Phys. Rev.*, 125:1067–1084, 1962.
- [34] Yuval Ne’eman. *Nucl. Phys.*, 26:222–229, 1961.
- [35] Yuval Ne’eman. *Phys. Lett.*, 82B:69, 1979.
- [36] G. Zweig. An SU(3) model for strong interaction symmetry and its breaking. Version 2. In D.B. Lichtenberg and Simon Peter Rosen, editors, *DEVELOPMENTS IN THE QUARK THEORY OF HADRONS. VOL. 1. 1964 - 1978*, pages 22–101. 1964.

- [37] H. David Politzer. *Phys. Rept.*, 14:129–180, 1974.
- [38] K. Shimizu and S. Yamazaki. *Phys. Lett.*, B390:1–6, 1997.
- [39] Kim Maltman and Nathan Isgur. *Phys. Rev. Lett.*, 50:1827, 1983.
- [40] R. K. Bhaduri. *MODELS OF THE NUCLEON: FROM QUARKS TO SOLITON*. 1988.
- [41] Stefan Scherer. *Adv. Nucl. Phys.*, 27:277, 2003.
- [42] M. L. Goldberger and S. B. Treiman. *Phys. Rev.*, 110:1178–1184, 1958.
- [43] Kenneth G. Wilson. *Phys. Rev.*, D10:2445–2459, 1974. [,45(1974)].
- [44] John B. Kogut and Leonard Susskind. *Phys. Rev.*, D9:3501–3512, 1974.
- [45] A. De Rujula, Howard Georgi, and S. L. Glashow. *Phys. Rev.*, D12:147–162, 1975.
- [46] V. B. Berestetskii, E. M. Lifshitz, and L. P. Pitaevskii. *QUANTUM ELECTRODYNAMICS*, volume 4 of *Course of Theoretical Physics*. Pergamon Press, Oxford, 1982.
- [47] Yoichiro Nambu. *Phys. Rev. Lett.*, 4:380–382, 1960.
- [48] J. Goldstone. *Nuovo Cim.*, 19:154–164, 1961.
- [49] Gerard 't Hooft. *Phys. Rept.*, 142:357–387, 1986.
- [50] Edward V. Shuryak and Jonathan L. Rosner. *Phys. Lett.*, B218:72–74, 1989.
- [51] N. I. Kochelev. *Sov. J. Nucl. Phys.*, 41:291, 1985. [Yad. Fiz.41,456(1985)].
- [52] A. A. Belavin, Alexander M. Polyakov, A. S. Schwartz, and Yu. S. Tyupkin. *Phys. Lett.*, B59:85–87, 1975.
- [53] M. Oka and S. Takeuchi. *Phys. Rev. Lett.*, 63:1780–1783, 1989.
- [54] M. Fukugita, Y. Oyanagi, and A. Ukawa. *Phys. Rev.*, D36:824, 1987.
- [55] K. Shimizu. *Rept. Prog. Phys.*, 52:1–56, 1989.
- [56] K. Shimizu. *Phys. Lett.*, B148:418–422, 1984.
- [57] John Archibald Wheeler. *Phys. Rev.*, 52:1083–1106, 1937.

- [58] M. Oka and K. Yazaki. *Prog. Theor. Phys.*, 66:556–571, 1981.
- [59] M. Oka and K. Yazaki. *Prog. Theor. Phys.*, 66:572–587, 1981.
- [60] M. Oka and K. Yazaki. *Int. Rev. Nucl. Phys.*, 1:489–567, 1984.
- [61] A. Le Yaouanc, L. Oliver, O. Pene, and J. C. Raynal. *HADRON TRANSITIONS IN THE QUARK MODEL*. 1988.
- [62] E. Oset, R. Tegen, and W. Weise. *Nucl. Phys.*, A426:456, 1984. [Erratum: *Nucl. Phys.*A453,751(1986)].